Journal of Experimental Botany, Vol. 76, No. 14 pp. 3984–4002, 2025
https://doi.org/10.1093/jxb/eraf202 Advance Access Publication 14 May 2025

RESEARCH PAPER

A DUF630 and 632 domains-containing protein, ZmNRL1, acts as a positive regulator of nitrogen stress response in maize

Chunyan Zheng[1,2,†], Hanjie Li[1,†], Yanfei Liu[1,†], Xiner Huang[1], Junting Han[1], Na Luo[1], and Faqiang Li[1,3,4,*]

[1] College of Life Sciences, South China Agricultural University, Guangzhou 510642, China
[2] Lushan Botanical Garden, Jiangxi Province and Chinese Academy of Sciences, Jiujiang 332900, China
[3] State Key Laboratory for Conservation and Utilization of Subtropical Agro-Bioresources, South China Agricultural University, Guangzhou 510642, China
[4] Guangdong Provincial Key Laboratory of Protein Function and Regulation in Agricultural Organisms, South China Agricultural University, Guangzhou 510642, China

* Correspondence: fqli@scau.edu.cn
† These authors contributed equally to this work.

Received 16 January 2025; Editorial decision 8 May 2025; Accepted 13 May 2025

Editor: Hideki Takahashi, Michigan State University, USA

Abstract

Nitrogen (N) is a key macronutrient whose availability often determines maize growth and productivity. Improving nitrogen use efficiency (NUE) is critical to increase maize yield while reducing N input and, more importantly, to alleviate environmental pollution. However, only a few genes have been exploited for maize NUE improvement thus far. Here, we identified 44 candidate genes associated with NUE-related traits by performing a genome-wide association analysis in a maize natural population. We further found that the natural variations in *ZmNRL1*, encoding a DUF630 and DUF632 domains-containing protein, strongly associated with chlorophyll content under N starvation. Loss of function of *ZmNRL1* reduced nitrogen content and weakened plant growth under hydroponic and soil conditions, whereas overexpression of *ZmNRL1* conferred better tolerance to N stress and elevated yields in transgenic maize and Arabidopsis. Comparative transcriptome analysis further revealed that ZmNRL1 has a broad impact on the expression of many N utilization and signaling genes. Moreover, we showed that ZmNRL1 anchored to the plasma membrane, probably through the dual lipid modifications of myristoylation and palmitoylation. Thus, we propose that ZmNRL1 is a key regulator of the adaptation response to N limitation in maize and could be a potential target for breeding high-yield maize with enhanced NUE.

Keywords: Arabidopsis, GWAS, maize, nitrogen starvation, nitrogen use efficiency (NUE), plasma membrane, *ZmNRL1*.

Introduction

Maize (*Zea mays* L.) is one of the most important cereal crops utilized as human food, animal feed, and raw material for various industrial applications (Palacios-Rojas *et al.*, 2020). Hence, a significant amount of nitrogen (N) fertilizer has been applied for its production (Ladha *et al.*, 2016). However, it is estimated that less than half of the applied N fertilizer is absorbed or

Abbreviations: CC, Chlorophyll content; CDR, Chlorophyll degradation rate; DUF, Domain of unknown function; GWAS, Genome-wide association study; InDel, Insertion/deletion; LD, Linkage disequilibrium; NRL, Nitrate Regulatory Gene 2-like; NRT, Nitrate transporter; NT-OL, N translocation from old leaves; NT-OLS, N translocation from old leaves and stems; NT-YL, N translocation to young leaves; NUE, Nitrogen use efficiency; SNP, Single nucleotide polymorphism.

utilized in crops (Coskun *et al.*, 2017; Huang *et al.*, 2021), and a large portion is lost to the environment (Lassaletta *et al.*, 2014). Excessive application of N fertilizer resulted in not only increasing agricultural cost, but also serious environmental pollution, such as soil acidification and water eutrophication (Guo *et al.*, 2010, 2021; Y.Q. Liu *et al.*, 2021). Thus, breeding maize cultivars with higher nitrogen use efficiency (NUE), which is usually defined as the total grain yield or biomass produced per unit of N applied, offers a practical approach to increase crop yield while alleviating environmental pollution by reducing the use of N fertilizer (Dong and Lin, 2020).

As a complex quantitative trait, plant NUE consists of multiple physiological processes involving N sensing, uptake, transport, assimilation, and remobilization, governed by genetic and environmental factors (Xu *et al.*, 2012; Krapp, 2015; Xu and Takahashi, 2020). During the past two decades, extensive studies in *Arabidopsis thaliana* and rice (*Oryza sativa*) have identified several key regulators in nitrate utilization and signaling which have potential for NUE improvement (Vidal *et al.*, 2020). One such key regulator is Arabidopsis nitrate transporter AtNRT1.1, also known as CHLORATE RESISTANT 1 (CHL1) and NPF6.3. AtNRT1.1 is a dual-affinity nitrate transporter that responds to different nitrate concentrations through phosphorylation by CBL-INTERACTING PROTEIN KINASE 23 (CIPK23) (Tsay *et al.*, 1993; Wang *et al.*, 1998; Ho *et al.*, 2009). OsNRT1.1B is a functional homolog of Arabidopsis AtNRT1.1 in rice, and its variation largely explains the difference in NUE between *indica* and *japonica* varieties (Hu *et al.*, 2019). Arabidopsis NIN-LIKE PROTEIN7 (AtNLP7) is another key component in regulating primary N response by initiating a rapid N response cascade (Alvarez *et al.*, 2020), which is activated by nitrate and then migrates from the cytoplasm to the nucleus to trigger downstream nitrate-responsive genes (Marchive *et al.*, 2013; Liu *et al.*, 2017). AtNLP7 was also found to act as a cytosolic nitrate sensor and could bind nitrate directly, resembling the bacterial nitrate sensor NreA (Marchive *et al.*, 2013; Liu *et al.*, 2017, 2022). The potential role of NLPs in enhancing crop NUE was demonstrated by rice OsNLP4, overexpression of which significantly increased yield by 30% and NUE by 47% as compared with non-transgenic rice (Wu *et al.*, 2021).

In addition, several transcription factors (TFs) have been identified through reverse genetics and system approaches to function in regulating nitrate signal transduction and nitrogen-responsive gene expression, such as LATERAL ORGAN BOUNDARY DOMAIN (LBD) 37/38/39, NAC DOMAIN CONTAINING PROTEIN4 (AtNAC4), SQUAMOSA-PROMOTER BINDING PROTEIN-LIKE 9 (AtSPL9), and TGACG SEQUENCE-SPECIFIC BINDING PROTEIN1/4 (AtTGA1/4) (Rubin *et al.*, 2009; Krouk *et al.*, 2010; Alvarez *et al.*, 2014; Vidal *et al.*, 2014). Using a similar forward genetic approach, Arabidopsis NITRATE REGULATORY GENE 2 (AtNRG2), a protein with two domains of unknown function (DUF630 and DUF632), was identified for reduced nitrate responses. AtNRG2 acts as a positive regulator of nitrate signaling and controls nitrate-induced expression of multiple nitrate transporters such as AtNRT1.1, and downstream TFs. AtNRG2 also forms a complex with AtNLP7 in the nucleus although it does not interfere with nuclear retention of the latter (Xu *et al.*, 2016).

Thus far, the molecular identification of maize key factors in nitrate utilization and signaling is still in its infancy. Recently, (Cao *et al.* 2024) showed that the maize NRT1.1 ortholog, ZmNRT1.1B, is responsible for root-to-shoot nitrate translocation. Using a combined transcriptome analysis and subcellular localization study, the authors revealed that ZmNRT1.1B facilitated the nuclear retention of ZmNLP3.1, and co-regulated the expression of many genes involved in nitrate signaling, cytokinin biosynthesis, and carbon metabolism. In addition, several maize homologs of Arabidopsis *NLP7*, such as *ZmNLP5*, *ZmNLP6*, and *ZmNLP8*, were reported as key regulators of nitrate signaling and N metabolism (Cao *et al.*, 2017; Ge *et al.*, 2020). *ZmNRG2.7* (*GRMZM2G142913*), one of 23 *NRG2-like* genes in maize, was found to play an essential role in N signaling and metabolism, and the overexpression of *ZmNRG2.7* in the Arabidopsis *atnrg2* mutant could restore its defect in responding to nitrate and increase biomass and NUE (Li *et al.*, 2024). However, the function of other maize *NRG2* genes and their contributions to NUE remain to be investigated.

In the present study, we investigated the performance of 296 maize inbred lines through hydroponic screening under N-limiting conditions. A total of 87 genetic variants, resolved to a total of 44 candidate genes, were significantly associated with six NUE traits through genome-wide association study (GWAS). One of the most significant variations occurs within a gene which encodes a DUF630/632 domains-containing protein with homology to Arabidopsis NRG2, and thus designated as *NRG2-like1* (*ZmNRL1*). Genetic analysis showed that loss of *ZmNRL1* reduced maize biomass, nitrate content, and nitrate reductase (NR) activity under N starvation conditions, while constitutive overexpression of *ZmNRL1* remarkably improved the tolerance to N stress in maize. Comparative transcriptome analysis revealed that *ZmNRL1* has a broad impact on the gene expression of a set of N utilization and signaling genes. In addition, overexpression of *ZmNRL1* in maize and Arabidopsis also improved its growth and yield under N-limiting conditions. These findings indicate that ZmNRL1 is a positive regulator modulating maize N starvation response and a potential candidate gene for improving crop NUE.

Materials and methods

Plant materials and growth conditions

Mazie *zmnrl1-e* and *zmnrl1-m* in the B73 background were purchased from the Maize EMS-induced Mutant Database (MEMD, http://maizeems.qlnu.edu.cn/, stock ID: EMS-095209) and ChinaMu mutant

database (http://chinamu.jaas.ac.cn; stock ID: *Zm00001d019173*: 20346698), respectively. The position of ethylmethane sulfonate (EMS)-induced mutagenesis in *zmnrl1-e* was verified by genomic PCR using a pair of gene-specific primers (see Supplementary Table S1 for primers) followed by Sanger sequencing. Homozygous *Mu* mutant plants were identified by PCR using the *Mu* TIR-specific primer Mu67 and a gene-specific primer. All mutant plants were backcrossed to the B73 background for three generations and then were self-pollinated to obtain homozygous lines. All maize seedlings were grown in a plant growth chamber under long-day conditions (16 h light/8 h dark), 25 °C, and 60% relative humidity.

The *A. thaliana* ecotype Col-0 was used in this study. All seeds were sterilized and sown on full-strength Murashige and Skoog (MS) medium [4.3 g l^{-1} MS powder, 1% (w/v) sucrose, 0.05% (w/v) MES, and 0.7% (w/v) agar, pH 5.7]. All Arabidopsis and tobacco seedlings were grown under long-day conditions, 22 °C, and 50% humidity.

For seedling N-limitation studies, hydroponically grown maize B73 inbred line, *zmnrl1* mutants, and *ZmNRL1-OE* lines at the V2 stage were washed with dH_2O three times and transplanted into modified Hoagland nutrient solution containing either 0, 0.15, or 15 mM NO_3^- (Li *et al.*, 2015).

For phenotyping analysis of N-starved soil-grown maize seedlings, maize seeds were germinated and grown in 2.0 liter plastic pots containing Jiffy soil without micronutrients and macronutrients (1137467-300) for treatment for 3 weeks. For detection of N-related traits of adult plants, V3-stage seedlings were transplanted into 25 liter pots containing 20 liters of soil, and each pot contained one plant. The pots were randomly arranged and were allowed to open pollinate. Plants were irrigated with 500 ml of modified Hoagland nutrient solution containing either 15 mM NO_3^- (high-N) or 0.15 mM NO_3^- (low-N) during the whole growth stage, and each treatment was repeated with three replications.

For phenotyping analysis of N-starved Arabidopsis seedlings, seeds of wild-type Col-0 and *ZmNRL1*-overexpressing (OE) lines were germinated and grown on full-strength MS agar medium for 7 d. Subsequently, seedlings were transferred into fresh MS agar medium containing 10 mM NO_3^- (high-N) or 0.1 mM NO_3^- (low-N). After 8 d treatment, plants were harvested and partitioned into above-ground parts and roots, and soluble protein content, nitrate content, and NR activity were measured.

For phenotyping analysis of N-starved mature Arabidopsis plants, 7-day-old seedlings were transferred into 0.5 liter plastic pots and irrigated with 1.0 liter of modified Hoagland nutrient solution containing either 10 mM NO_3^- (high-N) or 0.1 mM NO_3^- (low-N) every 3 d. Pictures were taken 3 weeks after treatment, and the above-ground parts were harvested for biomass measurement.

Experimental design and phenotypic data collection

A total of 296 maize accessions were used in this study (Fu *et al.*, 2013). All accessions were raised in a plant growth chamber at South China Agricultural University, China. A schematic flow diagram describing plant growth conditions, phenotyping, and sample collection is shown in Supplementary Fig. S1A. Briefly, the seeds were germinated and transplanted onto thermocol sheets fitted on 10 liter plastic containers filled with modified Hoagland nutrient solution (Li *et al.*, 2015). Each container was divided into 40 plots. All genotypes were randomly planted in triplicate, and at least six plants of each genotype were grown. When seedlings reached the V2 stage, the solution was replaced by N-free Hoagland solution (2 mM $MgSO_4{\cdot}7H_2O$, 1 mM KH_2PO_4, 0.02 mM Fe-EDTA, 5 mM $CaCl_2$, 2.8 mM KCl, 0.6 mM K_2SO_4, and micronutrient salts) for another 8 d.

The sample seedlings were harvested before and after N starvation. Each sample was partitioned into old leaves (the first and second leaves), young leaves (the third and younger leaves), stems, and roots, and dried at 105 °C for 30 min and then at 65 °C for 3 d, followed by N content measurement using an element analyzer (Elementar vario EL cube, German). The N-related indexes, namely N translocation from old leaves (NT-OL), N translocation to young leaves (NT-YL), and N translocation from old leaves and stems (NT-OLS), were calculated to assess N accumulation and partitioning. The chlorophyll content (CC) of the second leaf was measured using a hand-held chlorophyll meter (SPAD), and the chlorophyll degradation rate (CDR) was calculated as (CC before N starvation–CC after N starvation)/8×100%.

Genome-wide association study analysis

The 557 977 transcriptomic single nucleotide polymorphisms (SNPs) with MAF (minor allele frequency) ≥ 0.05 from the Maizego website (www.maizego.org/Resources.html) were used for GWAS analysis (Fu *et al.*, 2013). A general linear model (GLM, Q model) and a standard mixed linear model approach (MLM, Q+K model) were applied by TASSEL v5.0 (Bradbury *et al.*, 2007), in which the population structure (Q) and kinship (K) were estimated as previously described (Yang *et al.*, 2011). In addition, a Bonferroni-corrected threshold ($n = 1/557\,977$) was used as cut-off to identify significant associated SNPs. Quantile–quantile (Q–Q) plots and Manhattan plots were generated by using the CMplot R package to visualize significant SNP–trait associations (Yin *et al.*, 2021).

Analysis of *ZmNRL1*-based association with chlorophyll content

The resequencing *ZmNRL1* data of 43 maize inbred lines belonging to the population of 296 accessions were aligned to the B73 reference genome sequence (AGPv4). The ~4.6 kb genomic region, consisting of the 5'-untranslated region (UTR), coding regions, introns, and 3'-UTR sequences, was amplified using six pairs of primers designed based on the B73 genome sequences (Supplementary Table S1). The amplified sequences were assembled by SnapGene v3.2.1 software (https://www.snapgene.com/) and aligned by MEGA v6.0 (https://megasoftware.net/). The SNPs and insertion/deletions (InDels) (MAF ≥ 0.05) were identified and then used to perform marker–trait association with CC and to calculate the pairwise linkage disequilibrium (LD) using TASSEL v5.0.

Measurements of nitrate, protein contents, and nitrate reductase enzyme activity

Nitrate content and NR activity in maize seedlings and Arabidopsis were quantified using the methods described by Xu *et al.* (2016). Briefly, 0.4 g of fresh tissues was milled into powder and mixed with 10 ml of ddH_2O followed by boiling at 100 °C for 30 min, and centrifuged at 13 400 *g* for 10 min. The supernatant was used to measure the nitrate content using the salicylic acid method. For measurement of NR activity, 0.1 g of root and leaf tissues was homogenized in extraction buffer (5 mM EDTA-Na_2, 5 mM cysteine, 25 mM phosphate buffer, pH 7.5). Plant crude mixtures were collected and added to buffer (0.5 mg ml^{-1} NADH, 110 mM K_2HPO_4, 16 mM KH_2PO_4, and 100 mM KNO_3). After incubation for 40 min at 25 °C, the reaction solution was stopped by 1% sulfanilamide and 0.2% *N*-(1-naphthyl)-ethylenediamine hydrochloride, and measured at 540 nm. Soluble protein content was determined using the Bradford assay (Bradford, 1976). All experiments have been performed with three biological replicates.

Generation of transgenic maize and Arabidopsis plants overexpressing *ZmNRL1*

To generate transgenic maize plants overexpressing *ZmNRL1*, the full-length *ZmNRL1* cDNA was inserted into the *CPB-Ubipro:GFP* binary vector (Zhao *et al.*, 2023) digested with *Bam*HI driven by the maize

ubiquitin promoter to create the *ubipro:ZmNRL1-GFP* vector. The construct was then transformed into the embryo calli of maize inbred line B73 using the *Agrobacterium*-mediated transformation method (Ishida *et al.*, 2007). The positive transgenic lines were obtained by selection on Basta and confirmed by PCR analysis using *bar* gene-specific primers (Supplementary Table S1). Two independent T_2 homozygous lines were selected for further studies.

To generate transgenic Arabidopsis plants overexpressing *ZmNRL1*, the full-length *ZmNRL1* cDNA was cloned into *pGreenII* 0229 (https://www.snapgene.com/plasmids/plant_vectors/pGreenII_0229) digested with *Xho*I and *Spe*I enzymes driven by the cauliflower mosaic virus (CaMV) *35S* promoter to generate the *p35S:ZmNRL1-6HA* construct. The construct was then introduced into *Agrobacterium* strain GV3101 containing pSoup helper plasmid and transformed into Arabidopsis Col-0 using the floral dip method (Clough and Bent, 1998). More than six independent transgenic lines were obtained by Basta-based selection, and two T_3 homozygous lines were selected for further studies.

Subcellular localization assay

The subcellular localization studies using the tobacco transient expression system were performed as described previously by Luo *et al.* (2023). *ZmNRL1* cDNA was cloned into the *pEGAD-GFP* vector (accession no. AF218816) between the *Age*I and *Hin*dIII sites to generate an N-terminal fusion protein with green fluorescent protein (GFP; *35S:ZmNRL1-GFP*). The myristoylation-defective Gly-to-Ala (G2A) and palmitoylation-defective Cys-to-Ser (C3S) mutations were introduced into ZmNRL1 by one-step PCR using specific primers (Supplementary Table S1), and the corresponding PCR fragments were cloned into pEGAD-GFP to generate $ZmNRL1^{G2A}$–GFP, $ZmNRL1^{C3S}$–GFP, and $ZmNRL1^{G2AC3S}$–GFP variants. Subsequently, the constructs were introduced into the *Agrobacterium* strain GV3101. The ZmNRL1–GFP variants were transiently expressed in tobacco leaves. Confocal images were taken 36 h after agroinfiltration using a Leica STELLARIS 5 microscope (Leica, https://www.leica-microsystems.com/).

To detect ZmNRL1–GFP in stable transgenic maize plants, the plants were grown hydroponically under long-day conditions with Hoagland solution containing 4 mM NO_3^- for 7 d. Lateral roots were collected and incubated with 4 μM FM4-64 dye for 5 min and then washed with Hoagland medium before visualization. GFP was excited at 488 nm and detected at 500–520 nm, while FM4-64 was excited at 543 nm and detected at 560–640 nm. For co-localization imaging of GFP and FM4-64, multi-track line switching was used to avoid fluorescence bleedthrough.

Yeast two-hybrid assays

The full-length *ZmNRL1* was cloned into the pGBKT7 vector (Clontech, Palo Alto, CA, USA) between the *Bam*HI and *Eco*RI sites to generate the BD–ZmNRL1 construct. Meanwhile, full-length *ZmNLP5* (*Zm00001d015201*), *ZmNLP6* (*Zm00001d037786*), and *ZmNLP8* (*Zm00001d009017*) were amplified from cDNA synthesized from maize B73 leaf total RNA using gene-specific primers (Supplementary Table S1). The PCR products were then cloned into the pGADT7 vector between the *Bam*HI and *Eco*RI sites to obtain AD–ZmNLP constructs. The recombinant plasmids were co-transformed into the yeast strain Y2H Gold. The interactions between ZmNRL1 and ZmNLPs were determined by measuring the growth of transformants after 3 d on selective medium lacking Leu, Trp, His, and Ade.

RNA-sequencing assays

Ten-day-old maize seedlings were treated with modified Hoagland solution supplemented with 15 mM NO_3^- or 0.15 mM NO_3^- for 48 h, and root tissues were harvested for total RNA which was isolated using the RNAprep Pure kit (TIANGEN, Beijing, China). A total of 18 cDNA libraries of six samples (WT+N, *ZmNRL1-OE*+N, *zmnrl1-m*+N, WT–N, *ZmNRL1-OE*–N, and *zmnrl1-m*–N) with three repeats were constructed and sequenced using the Illumina NovaSeq 6000 platform by Biomarker Tech (Beijing, China). Raw data reads with 150 bp paired-ends were generated, and assessed by FastQC v0.11.9 software. Clean reads were then aligned to the Mazie genome B73 RefGen_v4 using the HISAT2 v2.2.1 program with default parameters. Fragment quantifications were computed with FeatureCounts v2.0.1 in paired-end mode. The analysis of differentially expressed genes (DEGs) was performed using the DESeq2 R packages v1.3.0 with a threshold of $\log_2$ (fold change) ≥ 1 and adjusted *P*-value ≤ 0.05. Gene Ontology (GO) term enrichment analysis was performed by the software agriGO v2.0.

Quantitative real-time PCR analysis

Total RNAs were isolated from various tissues of maize plants or Arabidopsis seedlings using the RNA plant Extraction Kit based on the manufacturer's protocol (Tiandz Inc., Beijing, China) and then reverse-transcribed into cDNA with the Hiscript II Q RT SuperMix for qPCR (+gDNA wiper) cDNA kit (Vazyme Biotech Co., Ltd, Nanjing, China). Quantitative real-time PCR (qRT-PCR) was performed using SYBR Green Mixture to detect gene expression. The maize ubiquitin ligase gene *ZmUBC* (*Zm00001d053838*) and the Arabidopsis actin gene *AtActin* (*At5g09810*) were used as the internal controls for maize and Arabidopsis qRT-PCR, respectively. Each sample was performed on three independent biological replicates. All qRT-PCR primers are listed in Supplementary Table S1.

Protein isolation and western blotting

Total protein was extracted by homogenizing maize or Arabidopsis tissues with 2:1 (v:FW) sample buffer [50 mM Tris–HCl pH 6.8, 50 mM DTT, 1% SDS, 0.005% bromophenol blue, 10% glycerol, and 10% (v/v) 2-mercaptoethanol]. The homogenized samples were then vortexed for 5 min, boiled at 95 °C for 5–10 min, and centrifuged at 12 000 *g* for 5 min to remove insoluble debris. The membrane and cytosol fractions were extracted using the Membrane and Cytosol Protein Extraction Kit (P0033, Beyotime, China). The protein extract was separated by 10% SDS–PAGE for immunoblot analysis. The antibodies against HA and GFP used in this study were purchased from Yeason (30702ES, Shanghai, China) and TransGene Biotech (HT801-01, Shanghai, China), respectively.

Sequence alignment and phylogenetic tree analysis

The full-length amino acid sequences of ZmNRL1 and its homologs from rice and Arabidopsis were downloaded from NCBI (http://www.ncbi.nlm.nih.gov/) and Ensemble plants (https://plants.ensembl.org/index.html). All sequences were aligned using MEGA v6.0 with default parameters. The Neighbor–Joining phylogenetic tree was constructed based on the aligned sequences with 1000 bootstrap replicates. The tree was visualized using the iTOL online website (https://itol.embl.de/).

Statistical analysis

Statistical values in this study were determined by two-tailed Student's *t*-tests and one-way ANOVA using SPSS 19.0 software. All figures were visualized by GraphPad Prism v8.0.2 and Adobe Illustrator CC 2019.

Results

Identification of candidate genes for nitrogen use efficiency in maize by genome-wide association study

To identify genetic components contributing to maize NUE, 296 representative inbred lines were selected to conduct a GWAS analysis (Fu *et al.*, 2013). Considering the complexity of plant NUE, which is affected by environmental factors and intensity of the stress imposed on plants, we decided to focus on the tolerance to severe N starvation at the seedling stage in environment-controlled growth chambers. Maize seedlings were pre-cultured with Hoagland solution containing sufficient N until the V2 stage, then transferred to N-free solution for 8 d (see the Materials and methods). Plants were collected before and after N starvation, partitioned into old leaves (the first and second leaves), young leaves (the third and younger leaves), stems, and below-ground parts to measure total N contents. Three indices, namely N translocation from old leaves (NT-OL), N translocation to young leaves (NT-YL), and N translocation from old leaves and stems (NT-OLS), were calculated. In addition, chlorophyll content (CC), as an indicator of N status of crops (Yuan *et al.*, 2016), chlorophyll degradation rate (CDR), and total dry weight (TDW) were also measured. We found substantial phenotypic variations within the population, ranging from complete senescence to lack of senescence of old leaves after N stress (Fig. 1A, B). All six NUE-related traits/indices exhibited wide phenotypic variations with approximately normal distribution (Supplementary Fig. S1B; Supplementary Tables S2, S3). Additionally, Pearson's correlation analysis revealed several significant pairwise correlations between these NUE-related traits. The values ranged from −0.91 between CC and CDR to 0.66 between NT-OL (or NT-YL) and TDW (Supplementary Fig. S1C; Supplementary Table S2). High to moderate broad-sense heritability (h^2) was observed for all six NUE-related traits, ranging from 92.91% for TDW to 52.35% for NT-OLS (Supplementary Table S3). The phenotypic variation analyses of the NUE-related traits for each subpopulation revealed that there was no noticeable difference among these four subpopulations, indicating that maize population structure has no effect on these traits (Supplementary Fig. S1D; Supplementary Table S2). Thus, the results indicated that the population was suitable for further association mapping to detect genetic components underlying maize NUE.

Using 557 977 SNPs with an MAF ≥ 0.05, we performed GWAS to identify genetic loci associated with NUE-related traits. In total, 87 significant SNP markers were identified which were located in 44 candidate genes using GLM and MLM (Supplementary Fig. S2; Supplementary Table S4). GO analysis indicated that 12 genes were involved in plant stress responses, including genes homologous to Arabidopsis regulators responding to cold stress (*At2g39810*, *HOS1*), salt stress (*At2g45660*, *SOC1*), and drought/salt stress (*AT1G78080*, *RAP2.4*) (Supplementary Fig. S3A; Supplementary Tables S4, S5). To determine whether the candidate genes functioned in response to N stress, their gene expression profiles in leaves under low N were retrieved from published RNA-seq data (SRP139303) (McLoughlin *et al.*, 2018). As shown in Supplementary Fig. S3B, we observed three genes up-regulated and three genes down-regulated significantly upon N stress in young leaves (the fourth leaves). In addition, four genes were up-regulated in old leaves (the second leaves) by low-N treatment. Together, the large proportion of genes involved in N metabolism and having altered expression under N starvation conditions indicate that our GWAS successfully identified genes critical for maize N utilization.

ZmNRL1 is significantly associated with maize seedling chlorophyll content under N starvation

We then selected candidate genes with GO annotation 'GO:1901698: Response to nitrogen compound' for further research. An SNP within *Zm00001d019173*, chr7.S_19754410, was identified to be significantly associated with CC under N starvation ($-\log_{10} 4.59\times10^{-7} = 6.3$), which explained ~8% of the phenotypic variation (Fig. 1C–E). *Zm00001d019173* encoded a protein containing a DUF630 at the N-terminus and a DUF632 at the C-terminus. There are 26, 20, and 16 DUF630/632 members in maize, rice, and Arabidopsis genomes, respectively. A phylogenetic tree constructed for Zm00001d019173 along with those DUF630/632 members identified two major clades and revealed that Zm00001d019173 shared a close phylogenetic relationship with the well-studied Arabidopsis AtNRG2 (Supplementary Fig. S4). Thus, we named this gene *ZmNRL1* (*NRG2-like 1*).

To explore the function of *ZmNRL1*, we firstly examined its expression profile using publicly available RNA-seq data (http://ipf.sustech.edu.cn/pub/zmrna/) and qRT-PCR analysis. As shown in Supplementary Fig. S5A and B, *ZmNRL1* is ubiquitously expressed in roots, leaves, internodes, meiotic tassels, ligules/collars, and whole seeds. Moreover, *ZmNRL1* expression was found to be up-regulated in leaf and root tissues under N-deficiency conditions (Supplementary Fig. S5C, D). In addition to N starvation, *ZmNRL1* expression could also be induced by multiple biotic and abiotic stresses, including drought, cold, and heat stresses, and infections by *Trichoderma virens*, *Tetranychus urticae*, and aphids, while it was down-regulated by *Fusarium graminearum* infection (Supplementary Fig. S5C). These data indicated that *ZmNRL1* may play an important role in response to environmental stresses in maize.

To further investigate whether the natural variation in *ZmNRL1* was associated with CC, we re-sequenced the *ZmNRL1* gene in 43 randomly selected inbred lines (Supplementary Table S6). A 4 694 bp genomic region, spanning from the 5'-UTR to the 3'-UTR was analyzed. A total of 59 SNPs and 91 InDels were identified. Three variations in the

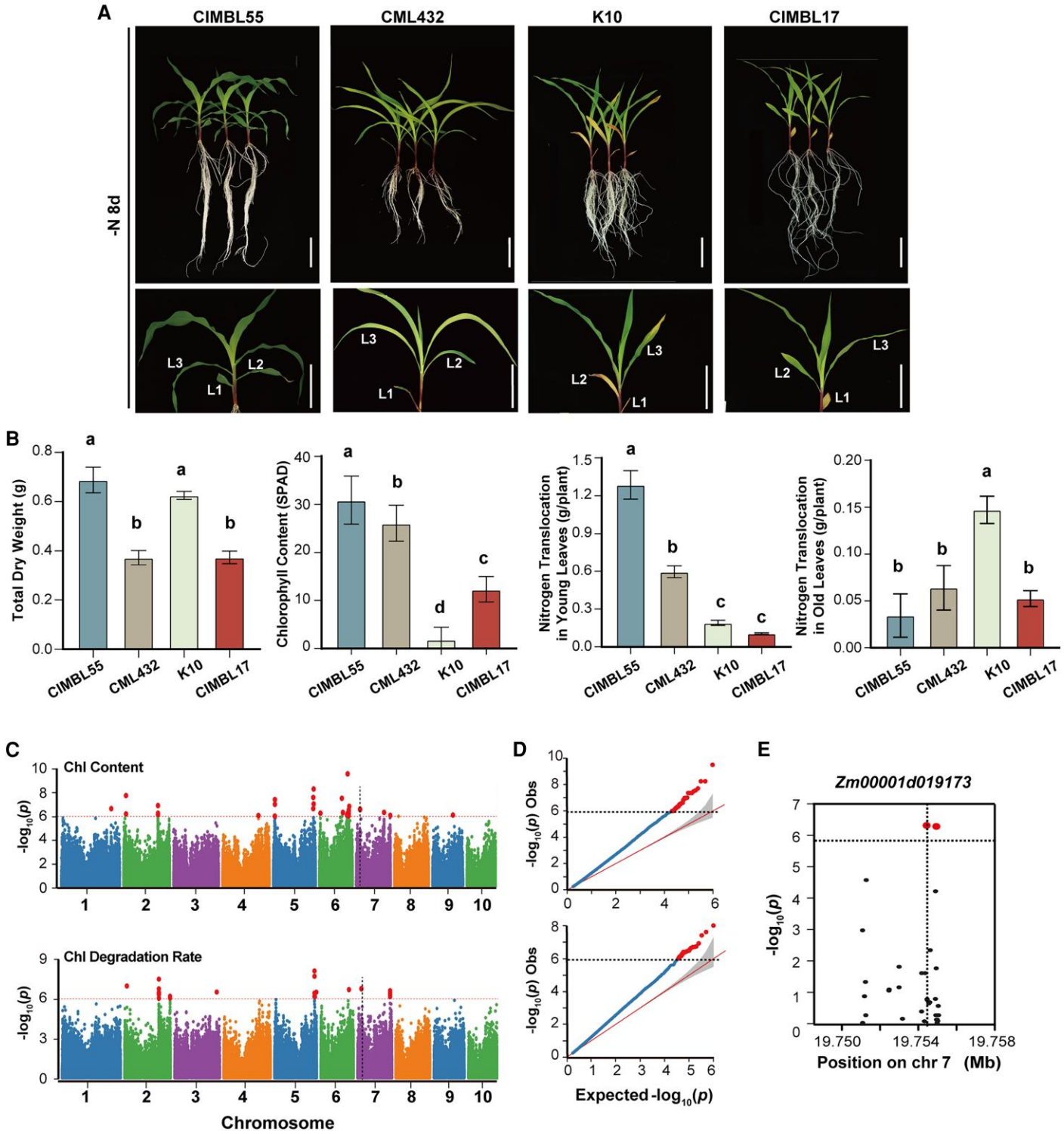

Fig. 1. GWAS of NUE-related traits in maize. (A) Representative images of contrasting growth phenotypes of four maize inbred lines under N-deficit conditions. Scale bars, 5 cm (top); 10 cm (bottom). (B) Analysis of total dry weight, chlorophyll content, nitrogen translocation in old leaves, and nitrogen translocation in young leaves from four maize inbred lines. Data show the means ± SD. Statistical significance was determined by one-way ANOVA followed by Turkey multiple comparison test at a P-value < 0.05. (C) Manhattan plots of chlorophyll content and chlorophyll degradation rate. GWAS was performed in a natural population consisting of 296 maize inbred lines using a general linear model (GLM). The dashed line depicts the significance threshold (1.79×10^{-6}), and the dots above dashed lines represent significant association SNPs. (D) Quantile-quantile plots for chlorophyll content and chlorophyll degradation rate. (E) Manhattan plot of the *Zm00001d01973* genomic region on chromosome 7. The lead SNPs are shown as dots above dashed line.

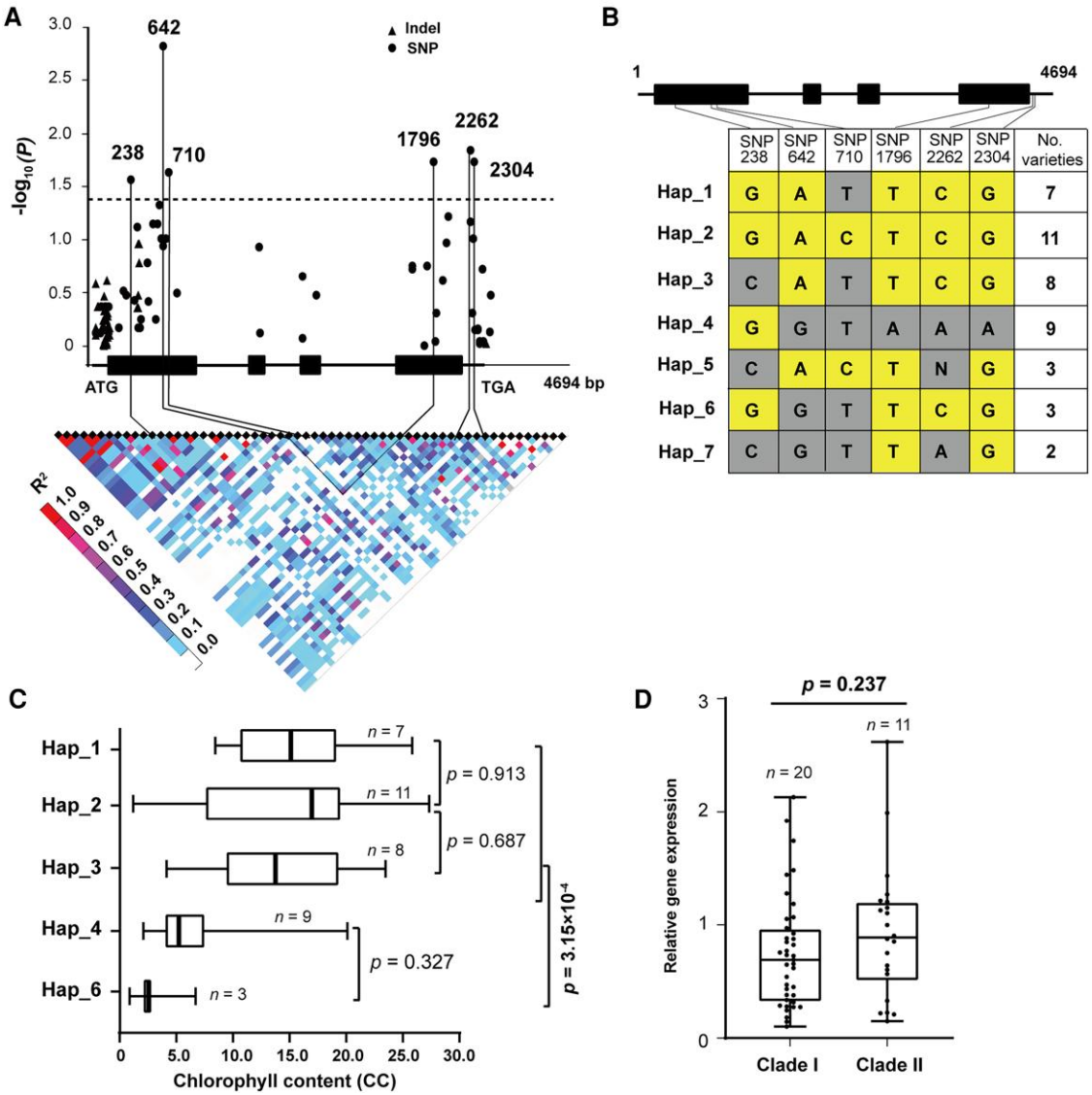

Fig. 2. Identification of *ZmNRL1* as a candidate gene involved in response to N starvation in maize. (A) Association study and LD analysis of *ZmNRL1* with the CC in a maize population. Triangles and dots represent SNPs and InDels, respectively. The 5'- and 3'-UTRs and introns of *ZmNRL1* are shown as black lines. Significantly associated SNP642 and SNP1796 are connected to the pairwise LD diagram by a solid line with $R^2 > 0.6$. (B and C) Haplotype analysis of *ZmNRL1*. *n*=the number of inbred lines in each haplotype. (D) Expression level of *ZmNRL1*. Selected inbred lines were treated with a N-free Hoagland solution for 2 h and the expression levels of *ZmNRL1* were then measured using qRT-PCR. Box-plots show the means ± SD from two independent experiments. *ZmUBC* was used as an internal control. Statistical significance was determined by two-sided *t*-test. *n*=the number of inbred lines in each genotype group.

first exon (SNP238, SNP642, and SNP710), one in the fourth exon (SNP1796/chr7.S_19754410), and two downstream of the coding region (SNP2262 and SNP2304) were found to be significantly associated with CC under N deficiency conditions (Fig. 2A). Two of these SNPs, SNP642 and SNP238, are non-synonymous variations, while all the other variations are synonymous SNPs. The most significant variation, SNP642, resulted in an amino acid residue change of asparagine into aspartic acid. Interestingly, it has strong LD with SNP1796/chr7.S_19754410 (LD, $R^2 > 0.6$), the variation identified previously. The other non-synonymous variation, SNP238, caused an alteration of serine to threonine. Based on these six variations, the 43 maize varieties were classified into seven haplotypes (Fig. 2B). $ZmNRL1^{B73}$ is a representative of Hap_2; Hap_5, Hap_6, and Hap_7 were minor haplotypes. These haplotypes mainly comprised two clades, with the inbred lines in Clade I (Hap_1, Hap_2, and Hap_3) having a statistically significant higher CC than those in clade II (Hap_4 and Hap_6, $P = 3.15 \times 10^{-4}$) (Fig. 2C). We further selected 20 accessions from Clade I and 11 accessions from Clade II randomly and analyzed the expression levels of *ZmNRL1* after low-N starvation. However, no significant difference in *ZmNRL1*

mRNA levels between the two clades was detected (Fig. 2D), indicating that the expression of *ZmNRL1* is not influenced by allele status at these SNPs.

Identification of maize mutants inactivating *ZmNRL1*

To better appreciate the importance of *ZmNRL1* in maize N utilization, we searched publicly available resources for mutants that would be likely to compromise functional expression. One allele, *zmnrl1-e*, was obtained from a gene-indexed collection of EMS-mutagenized maize lines (Lu *et al.*, 2018), and carried a single base substitution of C-to-T in exon 4, which led to premature termination of translation and destabilization of the *ZmNRL1* mRNA (Supplementary Fig. S6A, E). The other allele, *zmnrl1-m*, was identified from a ChinaMu library (Liang *et al.*, 2019) and carried a *Mu* insertion in the first exon (at 1084 bp after ATG) (Supplementary Fig. S6B, C). RT-PCR revealed that the *Mu* insertion blocked transcription across the insertion site as well as the full-length transcript (primers listed in Supplementary Table S1; Supplementary Fig. S6D). qRT-PCR analysis further showed that the *zmnrl1-m* mutant accumulated a considerably low level of transcript containing sequences downstream of the insertion sites (Supplementary Fig. S6E). Consequently, *zmnrl1-m* plants might express at most only a short fragment encompassing the C-terminal region of ZmNRL1, including the DUF632 domain.

Loss of *ZmNRL1* dampened the tolerance to N deprivation in maize seedlings

To evaluate the impact of the *zmnrl1* mutations on maize N utilization, we studied their growth and development under both N-rich and N-poor conditions. Both mutants were hydroponically cultured with N-rich or N-poor media for 11 d along with the wild-type B73 inbred line. Under N-rich conditions (15 mM NO_3^-), *zmnrl1* mutants appeared relatively normal phenotypically (Fig. 3), but their leaves were slightly less green and they exhibited a shorter fourth leaf relative to B73 (Fig. 3A–D). No significant differences were observed between *zmnrl1* mutants and B73 in terms of total dry matter (Fig. 3E).

Under low-nitrate (0.15 mM NO_3^-) or nitrate-free (0 mM NO_3^-) conditions, the growth and development of *zmnrl1* mutants were severely challenged as compared with wild-type plants. Enhanced leaf senescence was clearly evident for *zmnrl1* mutants as early as 6 d after N starvation and was more pronounced after 8 d of treatment (Fig. 3B, C). Additionally, the length of the fourth leaf of *zmnrl1* mutants was significantly shorter than that of B73 under nitrate-limiting conditions. When compared with the wild type, the dry matter production was decreased 8.29–16.77% and 35.04–55.21% in N-limited solutions for *zmnrl1-e* and *zmnrl1-m* mutants, respectively (Fig. 3E). Similarly, when grown on soil supplemented with low-nitrate or nitrate-free solutions, both *zmnrl1* mutants displayed accelerated leaf senescence, and their leaf CC and above-ground DW decreased more significantly as compared with the wild type (Supplementary Fig. S7).

To determine whether the *ZmNRL1* mutations impact maize leaf protein content, we examined the protein profiles of old leaves of *zmnrl1* mutants. As shown in Fig. 4A and Supplementary Fig. S8, both *zmnrl1* mutants displayed similar protein contents to that of the wild type under N-rich conditions, but had less protein accumulation under N deficiency conditions. Consistent with the phenotypic observations above, the protein degradation in older leaves of *zmnrl1* mutants was dramatically faster than that in the wild type as judged by SDS–PAGE, especially treatment for 8 d (Supplementary Fig. S8). We then measured the nitrate contents and NR activities of *zmnrl1* mutants. When grown with high-N solutions, *zmnrl1* mutants exhibited no significant difference in nitrate contents for both root and shoot tissues, whereas the nitrate contents and NR activities in both tissues were markedly decreased in *zmnrl1* mutants after N starvation (Fig. 4B–E). Collectively, the data indicated that *ZmNRL1* is essential for the tolerance of maize seedlings to N starvation.

Overexpression of *ZmNRL1* enhanced the tolerance of maize seedlings to N starvation

To further investigate the physiological properties of *ZmNRL1* in regulating the maize N starvation response, we generated maize transgenic lines constitutively expressing a *ZmNRL1-GFP* fusion under the control of maize *Ubiquitin* (*Ubi*) promoter in the B73 background, and two independent transgenic maize lines were chosen for further study. qRT-PCR analysis and western blot analysis with anti-GFP antibodies indicated that the *ZmNRL1-GFP* fusion was overexpressed in both lines (Supplementary Fig. S9A and B).

The *ZmNRL1-GFP-OE* lines exhibited a better tolerance to N limitation than the segregated non-transgenic control. Under N-deficiency conditions, *ZmNRL1-GFP-OE* lines displayed a delayed-senescence phenotype (Fig. 5A–C). Consistently, higher protein contents of old leaves (L1 and L2), and increased nitrate contents and NR activities in both root and leaf tissues were observed as compared with the wild type (Fig. 5G–K). In addition, *ZmNRL1-GFP-OE* lines showed stronger root systems during N limitation, which were ~0.308 g and ~0.483 g heavier than that of the wild type for *ZmNRL1-OE19* and *ZmNRL1-OE111*, respectively. The above-ground biomass was also significantly increased in *ZmNRL1-OE* plants compared with the wild-type plants (Fig. 5D, E). Consistently, the dry weights of *ZmNRL1-OE* plants were increased under low-N conditions (Fig. 5F). Similarly, when grown on soil supplemented with low-N solutions, *ZmNRL1-GFP-OE* lines performed better than the wild type, as evident by the higher biomass in both below-ground and above-ground portions (Supplementary Fig. S9C–F).

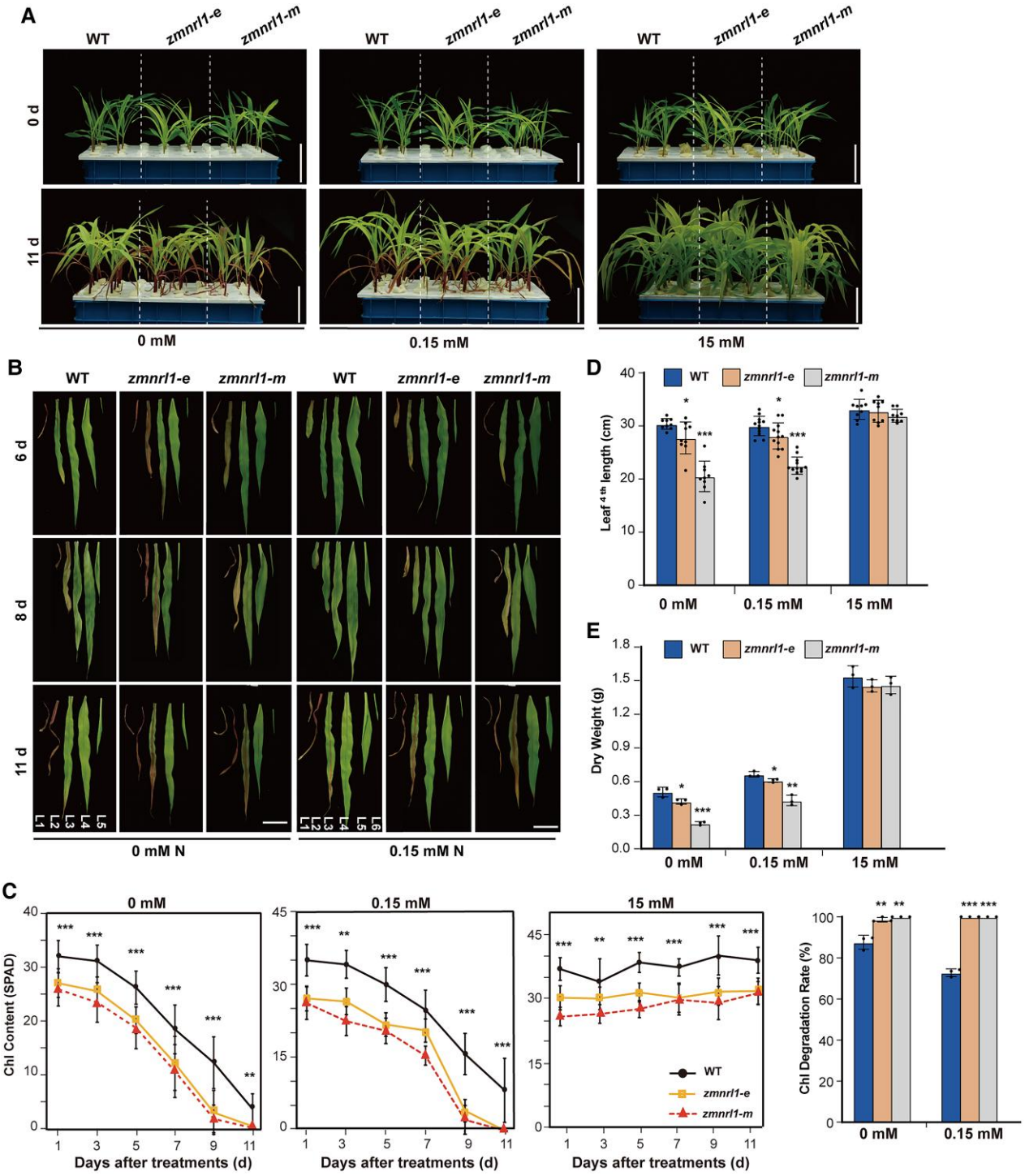

Fig. 3. Maize *zmnrl1* mutants are hypersensitive to N stress. (A) Phenotypic analysis of the maize B73 inbred line (WT), *zmnrl1-e*, and *zmnrl1-m* plants grown hydroponically under various N concentrations for 11 d. Maize seeds were germinated and grown to the V2 stage, then transferred to Hoagland solutions containing different concentrations of KNO_3 (0, 0.15, or 15 mM) for 11 d. Scale bar, 10 cm. (B) Leaf senescence phenotypes of WT, *zmnrl1-e*, and *zmnrl1-m* after N starvation. Images were taken at 6, 8, and 11 d after treatment. Scale bar, 10 cm. (C) Leaf chlorophyll contents and chlorophyll degradation rates, (D) the lengths of the fourth leaf, and (E) dry weights of the WT, *zmnrl1-e*, and *zmnrl1-m*. Data are shown as means ±SD. Statistical significance was determined by two-sided *t*-test. Asterisks indicate a significant difference between the WT and the *zmnrl1* mutants: $^{*}P < 0.05$, $^{**}P < 0.01$, and $^{***}P < 0.001$.

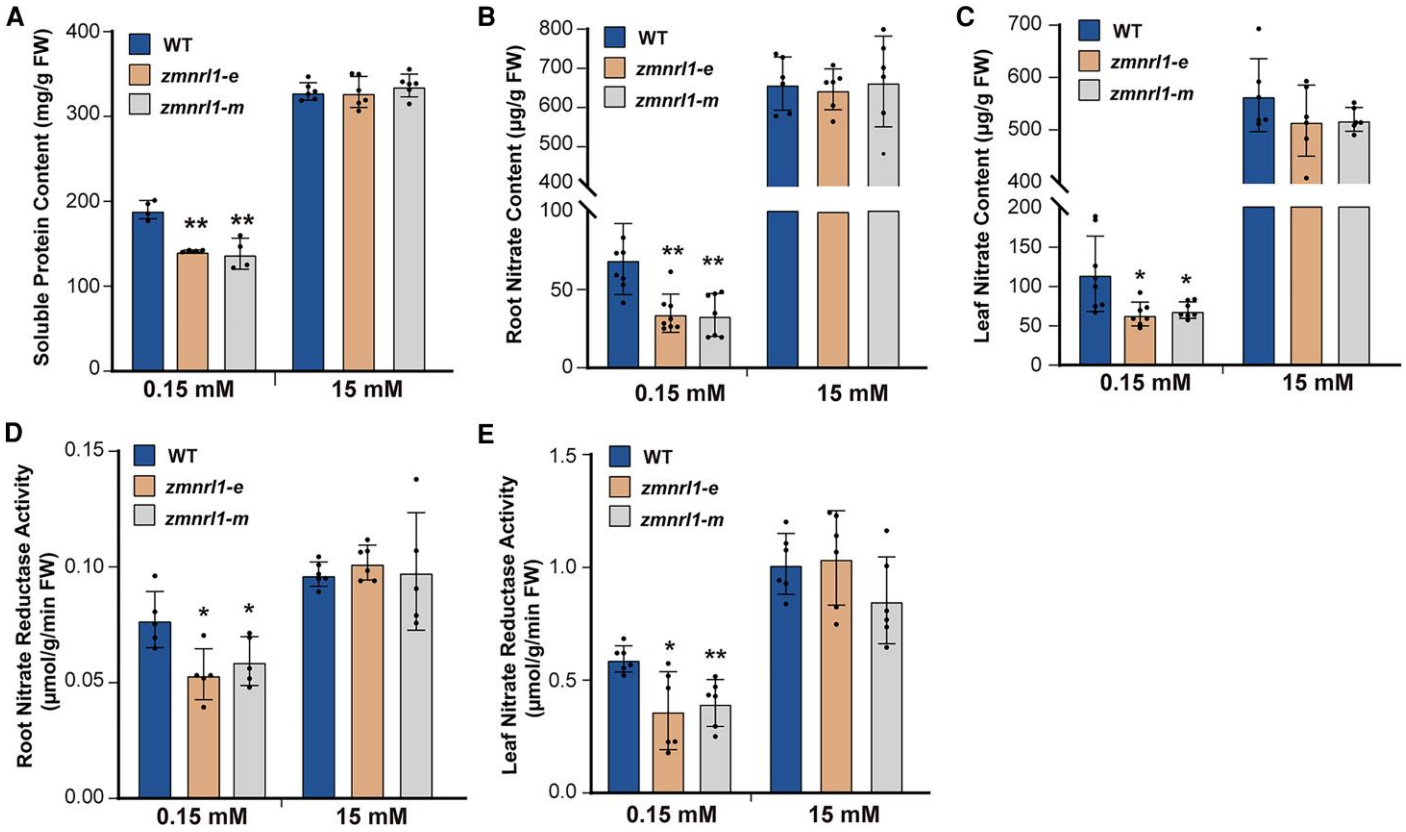

Fig. 4. Effects of the *zmnrl1* mutation on leaf protein content, nitrate content, and NR activity under N starvation conditions. (A) Quantitative measurement of the leaf soluble protein contents of wild-type (WT), *zmnrl1-e*, and *zmnrl1-m* leaves. (B, C) Quantitative analysis of the nitrate contents of root and old leaf tissues, respectively. (D, E) Quantitative measurement of the NR activities of root and leaf tissues, rexpectively. Data are shown as means ±SD. Statistical significance was determined by two-sided *t*-test. Asterisks indicate a significant difference between the WT and the *zmnrl1* mutants: * $P < 0.05$ and ** $P < 0.01$.

ZmNRL1 is required for the expression of N utilization genes

To further assess the role of *ZmNRL1* in NUE, we performed transcriptome sequencing analysis (RNA-seq) of 10-day-old wild-type, *zmnrl1-m*, and *ZmNRL1-OE111* seedlings after treatment with either 15 mM or 0.15 mM NO_3^- for 48 h. Principal component analysis (PCA) showed that both genotype and nutrient starvation profoundly affected the transcription profiles of maize seedlings (Supplementary Fig. S10A). In total, 1012 (756 up-regulated, 256 down-regulated), 1326 (702 up-regulated, 624 down-regulated), and 1214 (874 up-regulated, 340 down-regulated) DEGs were identified in the roots of the wild type, *zmnrl1-m*, and *ZmNRL1-OE111*, respectively (Supplementary Datasets S1–S3). GO term analysis of wild-type DEGs revealed that genes involved in N transport and metabolism are significantly enriched, including response to nitrate (GO:0010167), nitrogen cycle metabolic process (GO:0071941), nitrate transport (GO:0015706), nitrogen compound transport (GO:0071705), nitrate metabolic process (GO:0042126), nitrate assimilation (GO:0042128), response to nutrient levels (GO:0031667), and nitrate transmembrane transporter activity (GO:0015112), which accurately reflected the response of maize seedlings to N starvation (Supplementary Dataset S1).

To reveal how ZmNRL1 influences the expression of N utilization genes, we cross-compared the wild-type DEGs with those identified from mutated and overexpression lines. The combined survey revealed that 237 genes were induced by N starvation regardless of ZmNRL1 function, which included a number of genes involved in N transport, metabolism, and signaling, such as high-affinity nitrate transport-related genes (*ZmNRT2.5* and *ZmNRT2.7*), an ammonium transporter (*Zm00001d034782*), a urea–proton symporter (*ZmDUR3*), and N-related TFs (*ZmTGA4*, *ZmNLP7*, and *ZmNF-YA13*) (Fig. 6A, B; Supplementary Datasets S4, S6). In addition, 172 genes were found to be induced by N starvation in the wild type and *ZmNRL1-OE111* but not in *zmnrl1-m* plants, which were enriched in nutrient-related GO terms including 'transport', 'starvation', 'nutrient levels', and 'nitrogen.' (Fig. 6B; Supplementary Datasets S4, S6). The genes included well-known high-affinity nitrate transport-related genes *ZmNRT2.1* and *ZmNRT2.2*, nitrate

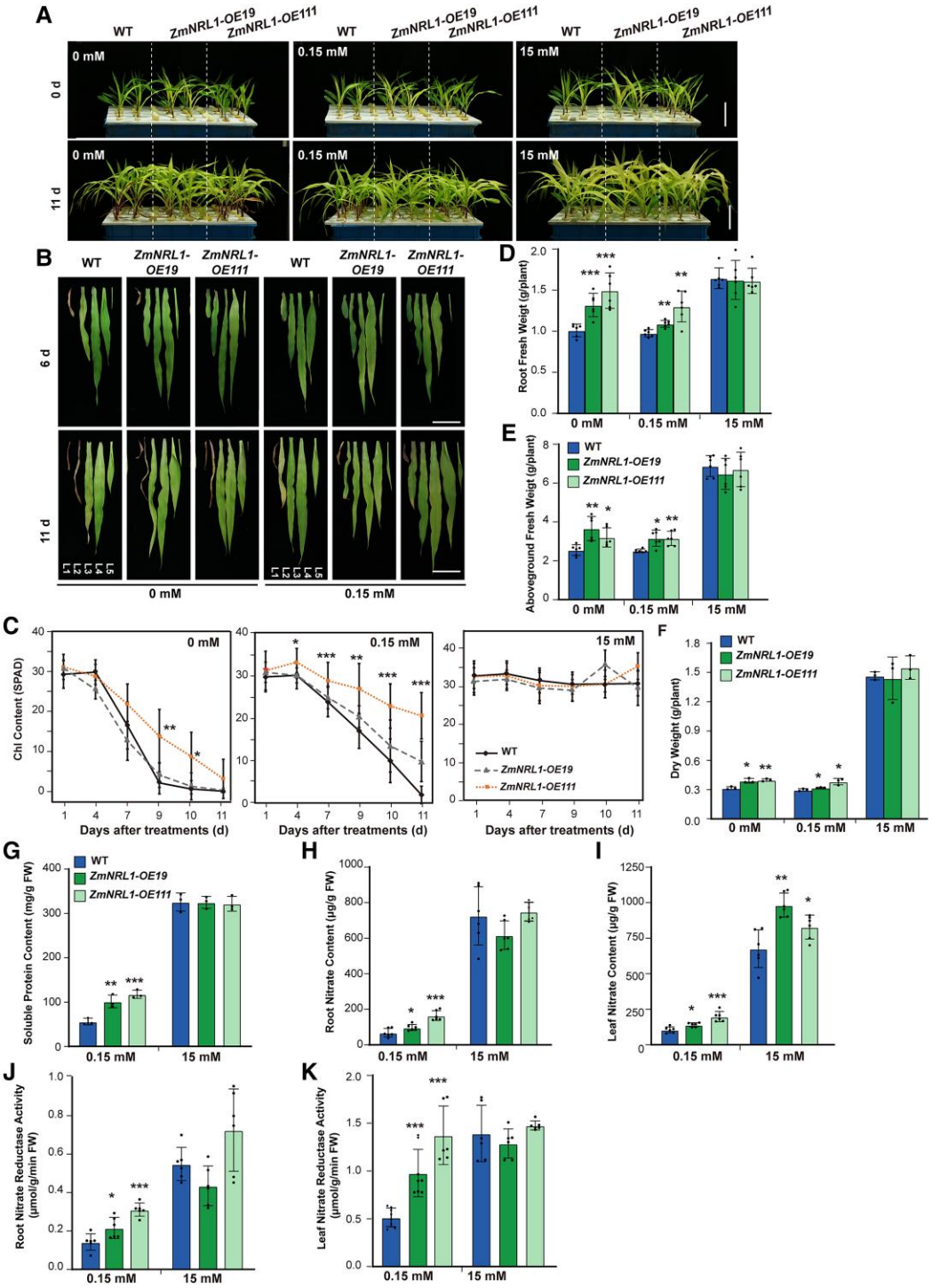

Fig. 5. Overexpression of *ZmNRL1* improves the tolerance of maize seedlings to N starvation. (A, B) Phenotypic analysis of *ZmNRL1*-overexpressing transgenic plants (*OE19* and *OE111*) grown hydroponically under various N concentrations. Maize seeds were germinated and grown to the V2 stage, then transferred to Hoagland solutions containing different concentrations of KNO_3 (0, 0.15, or 15 mM). Scale bar, 10 cm (A); 6 cm (B). (C) Chlorophyll content of the second leaf. Asterisks indicate a significant difference between the wild type (WT) and the two overexpression lines. (D-F) The fresh weights of root (D) and above-ground tissues (E), and dry weight per plant (F). Data in (D) and (E) were obtained from two independent experiments, each containing three biological replications. (G-K) Measurements of the soluble protein content of old leaf (L1 and L2, G), nitrate contents (H, I), and NR activities (J, K) of root and old leaf in *ZmNRL1*-overexpressing lines under different N conditions. Data are shown as means ±SD. Statistical significance was determined by two-sided *t*-test. Asterisks indicate a significant difference between the WT and the *ZmNRL1* overexpression lines: $^{*}P < 0.05$, $^{**}P < 0.01$, and $^{***}P < 0.001$.

transporter1/peptide transporter family genes *ZmNPF8.14* and *ZmNPF8.22*, and N-related TF genes *ZmNLP3* and *ZmCIPK23* (Fig. 6A). Interestingly, we also identified 349 genes up-regulated only in *ZmNRL1-OE111* plants upon N starvation, which were significantly enriched in categories involved in responses to stimulus, starvation, nutrient levels, and nitrate (Fig. 6B; Supplementary Dataset S4). Consistent with the comparison analysis of DEGs, genes involved in N responses, nitrogen signal transduction, and flavonoid biosynthesis showed lower expression levels in *zmnrl1* mutants than those in the wild type and *ZmNRL1-OE111* lines, whereas genes involved in hormone signaling had higher transcript abundance in the mutant (Fig. 6C). qRT-PCR analysis further confirmed that the expression levels of N stress-induced genes, including *ZmNRT2.1*, *ZmNRT2.2*, and *ZmASN4* (*asparagine synthetase 4*), were significantly increased in *ZmNRL1-OE111* and the wild type but not in *zmnrl1-m* (Fig. 6D). This significant enrichment in N starvation-inducible genes in the roots of *ZmNRL1-OE* ($P = 9.4e\text{-}05$, FDR = 0.02) suggests that ZmNRL1 acts as a positive regulator modulating the maize N starvation response. We also identified 101 genes that were down-regulated by N starvation regardless of ZmNRL1 function, which included well-known transcriptional repressors of the N starvation response, *ZmNIGT1.1* and *ZmNIGT1.2*, and an N transporter *ZmNPF5.10*, as well as nitrite reductases *ZmNiR1* and *ZmNiR2* (Supplementary Fig. S10B, C; Supplementary Datasets S5, S6).

ZmNRL1 is a plasma membrane protein

Like Arabidopsis AtNRG2, ZmNRL1 also contains two domains of unknown function, DUF630 and DUF632. Interestingly, AtNRG2, ZmNRL1, and other DUF630/632 domains-containing proteins in Arabidopsis and maize all contain a predicted myristoylation site (Gly2) while most also have a putative palmitoylation site (Cys3) at the N-terminus (Supplementary Fig. S11). To investigate the subcellular localization of ZmNRL1, we generated ZmNRL1–GFP, the ZmNRL1^{G2A}–GFP variant harboring a Gly-to-Ala substitution (G2A) in the predicted myristoylation site, the ZmNRL1^{C3S}–GFP variant containing a Cys-to-Ser substitution (C3S) in the predicted palmitoylation site, and the non-*N*-myristoylated and non-palmitoylated variant ZmNRL12^{G2AC3S}–GFP. When transiently expressed in tobacco leaf epidermal cells, ZmNRL1–GFP appeared to be predominantly anchored to the plasma membrane, which had a thin, sharp line of intense fluorescence along the cell periphery, while ZmNRL1^{G2A}, ZmNRL1^{C3S}, and ZmNRL1^{G2AC3S} proteins showed both cytosolic and nuclear localizations (Fig. 7A). Consistently, the plasma membrane-resident pattern of ZmNRL1–GFP was also observed in the root cells of transgenic Arabidopsis and maize lines, as demonstrated by the co-localization of ZmNRL1–GFP with membrane dye FM4-64 (Fig. 7B, E), whereas ZmNRL12^{G2AC3S}–GFP showed a diffuse GFP distribution in the cytosol and nucleus in transgenic Arabidopsis root cells (Fig. 7B). Interestingly, when plants were grown under N-poor conditions, the Arabidopsis seedlings expressing either *ZmNRL1-GFP* or *ZmNRL1^{G2AC3S}-GFP* all showed a delayed leaf senescence phenotype as compared with the wild type (Fig. 7C, D), indicating that both could improve the tolerance of transgenic Arabidopsis to N starvation

We further examined the changes of the protein level and subcellular localization of ZmNRL1–GFP fusion upon N starvation. Consistent with the confocal microscopic observations, ZmNRL1–GFP was detected exclusively in the membrane fraction in cell fractionation experiments (Fig. 7F, G). Upon N starvation, the subcellular localization of ZmNRL1 appeared unchanged, but its protein level decreased significantly compared with unstressed plants (Fig. 7F, G). Therefore, these results clearly showed that ZmNRL1 anchored to the plasma membrane probably through the dual lipid modifications of myristoylation and palmitoylation, and its distinct localization profile from nucleus-localized AtNRG2 may indicate that the mechanism of ZmNRL1 in regulating N starvation-responsive genes differs from that of AtNRG2.

Overexpression of *ZmNRL1* improves maize yield and nitrogen use efficiency

To further evaluate the potential contribution of *ZmNRL1* to yield under N-limiting conditions, we planted wild-type, *zmnrl1* mutant, and *ZmNRL1-OE* lines in high-N and low-N soils as described in the Materials and methods. As shown in Fig. 8A–C, under low-N conditions, the above-ground biomass and root FW of *ZmNRL1-OE* lines were significantly higher than those of the wild type, while the biomass of *zmnrl1-m* was markedly less under similar growth conditions. Furthermore, *ZmNRL1-OE* lines showed an improved NUE under low-N conditions; the total N contents in the roots, ear leaves, and kernels of *ZmNRL1-OE* lines were all elevated as compared with the wild type (Fig. 8D–G).

Subsequently, we performed a field trial for *zmnrl1* mutant and *ZmNRL1-OE* overexpression plants under normal field conditions. As shown in Fig. 8H–K, *ZmNRL1-OE* had a growth advantage over the wild type in terms of plant heights and biomass, while both traits decreased in *zmnrl1-m* (Fig. 8I). In addition, when compared with the wild type, *ZmNRL1-OE* lines had heavier 100-kernel weight and higher grain yield per plant, while grain yield was decreased in the *zmnrl1-m* mutant (Fig. 8K). These data further implied the crucial roles of *ZmNRL1* in maize NUE and yields.

Heterologous expression of *ZmNRL1* confers tolerance to N deficiency

Considering the possible functional conservation of DUF630/632 domains-containing proteins between maize and Arabidopsis, we postulated that heterologous expression of

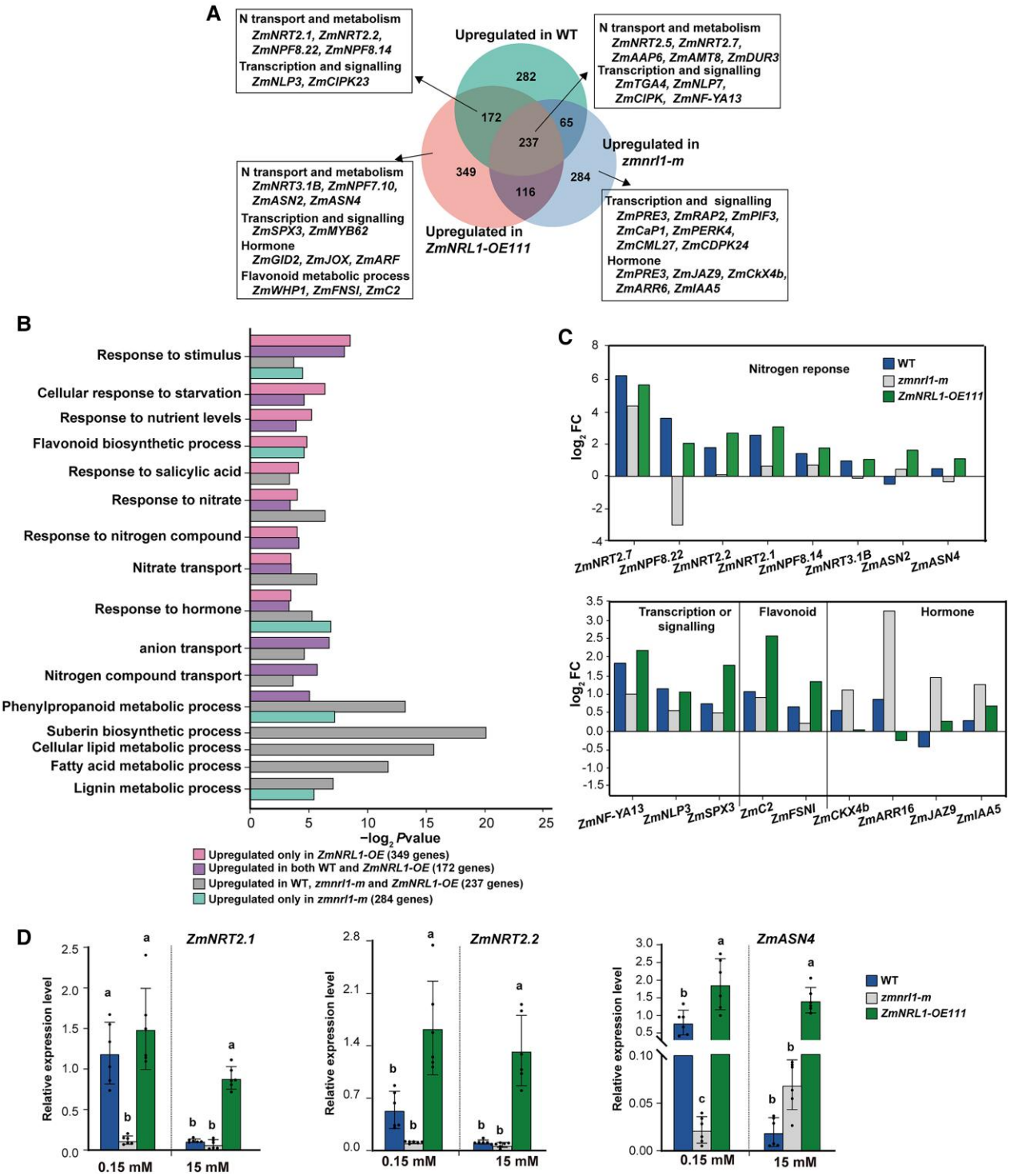

Fig. 6. *ZmNRL1* regulates the expression of N starvation-induced genes. (A) A Venn diagram showing the number of common and specific DEGs up-regulated by N starvation in the wild type (WT), *zmnrl1-m*, and *ZmNRL1-OE111*. (B) GO analysis of up-regulated DEGs showing the significant enrichment (FDR < 0.05) in the 'Biological Process' subcategories in each group based on Venn diagrams. Full results of GO enrichment analysis in each group are shown in Supplementary Dataset S4. (C) Representative genes from specific GO subcategories are expressed differentially in the WT, *zmnrl1-m*, and *ZmNRL1-OE111* upon N starvation. (D) qRT-PCR analysis of key genes involved in N utilization in WT, *zmnrl1-m*, and *ZmNRL1-OE111* plants. *ZmActin* was used as internal control. Bars show means ±SD of six biological replications from two independent experiments. Statistical significance was determined by one-way ANOVA followed by Turkey multiple comparison test at $P < 0.05$.

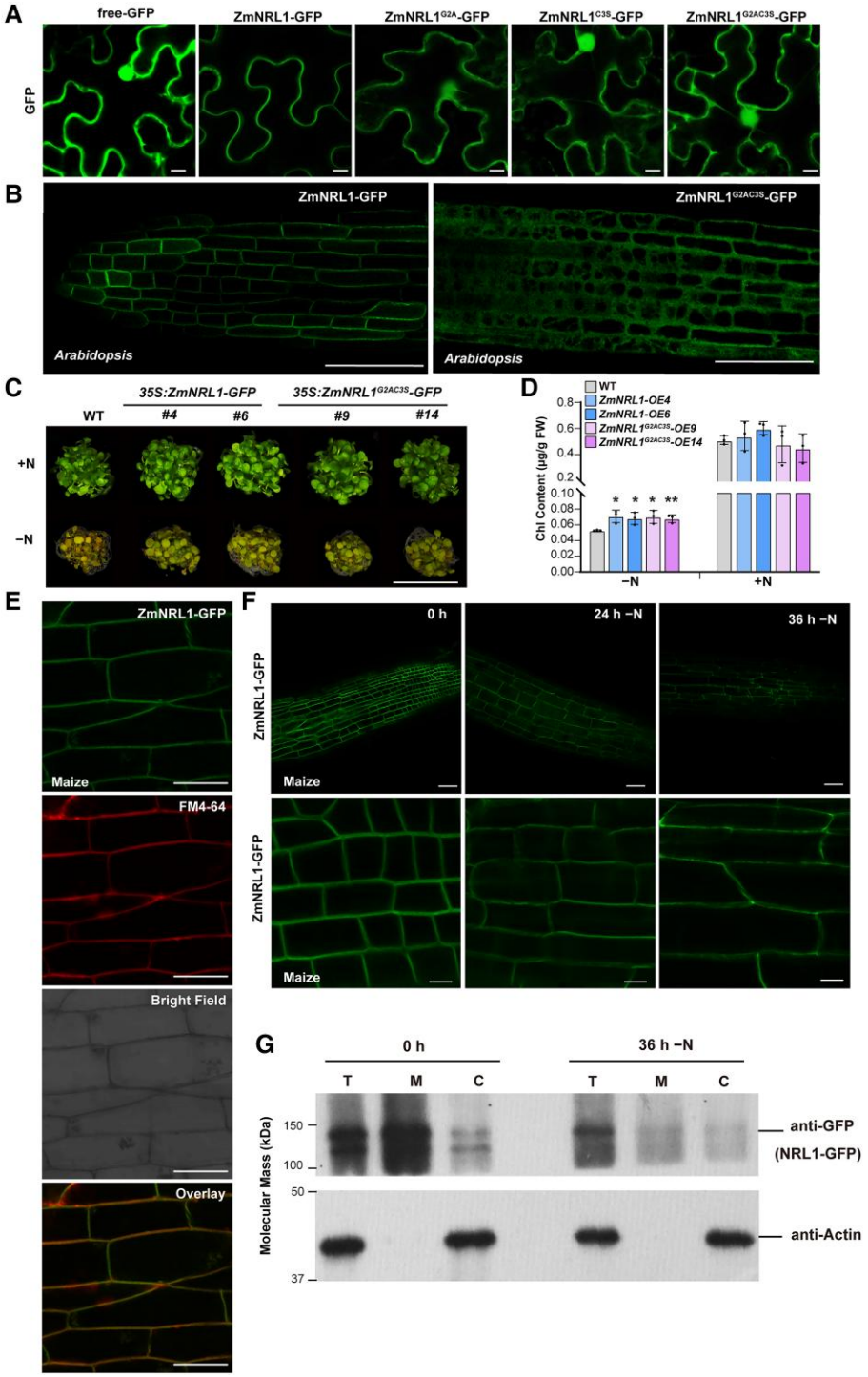

Fig. 7. The targeting of ZmNRL1 to the plasma membrane depends on its putative *N*-myristoylation and palmitoylation motifs. (A) The subcellular localizations of GFP-tagged ZmNRL1 and its variants. GFP-tagged wild-type ZmNRL1, non-*N*-myristoylated variant ZmNRL1^{G2A}, non-*S*-acylated variant ZmNRL1^{C3S}, and non-N-myristoylated and non-*S*-acylated variant ZmNRL1^{G2AC3S} were prepared and transiently expressed in tobacco epidermal cells. Bars, 10 μm. (B) Confocal imaging of the root cells of transgenic Arabidopsis expressing *35S:ZmNRL1-GFP* and *35S:ZmNRL1^{G2AC3S}-GFP*. Bars, 50 μm. (C and D) Phenotypes of *35S:ZmNRL1-GFP* and *35S:ZmNRL1^{G2AC3S}-GFP* lines grown under low-N conditions. All plants were germinated and grown on MS medium for 7 d and then transferred to MS liquid medium without nitrogen (-N). Plants were photographed after 8 d of N starvation. Bars, 3 cm. Total chlorophyll contents of plants are shown in (D). Data are shown as means ±SD. Statistical significance was determined by two-sided *t*-test. Asterisks indicate a significant difference between the WT and the *ZmNRL1-GFP* or *ZmNRL1^{G2AC3S}-GFP* lines: $^{*}P < 0.05$ and $^{**}P < 0.01$. (E) Confocal images of transgenic maize root cells from 10-day-old *ZmNRL1-GFP-OE111* seedlings stained with FM4-64. Bars, 25 μm. (F) Subcellular localization of ZmNRL1 under N-deficient conditions. Seeds were germinated and grown on N-rich medium for 10 d, then analyzed with confocal microscopy 24 h or 36 h after N starvation. Partial enlargement of the figure is shown at the bottom. Bars, 50 μm (top); 10 μm (bottom). (G) Western blot analyses of ZmNRL1-GFP. Total (T), membrane (M), or cytosolic (C) protein extracts were prepared from ZmNRL1-GFP transgenic plants 36 h after N starvation. Immunodetection was performed with antibodies against GFP to detect ZmNRL1-GFP, and anti-actin antibody as a cytoplasmic marker.

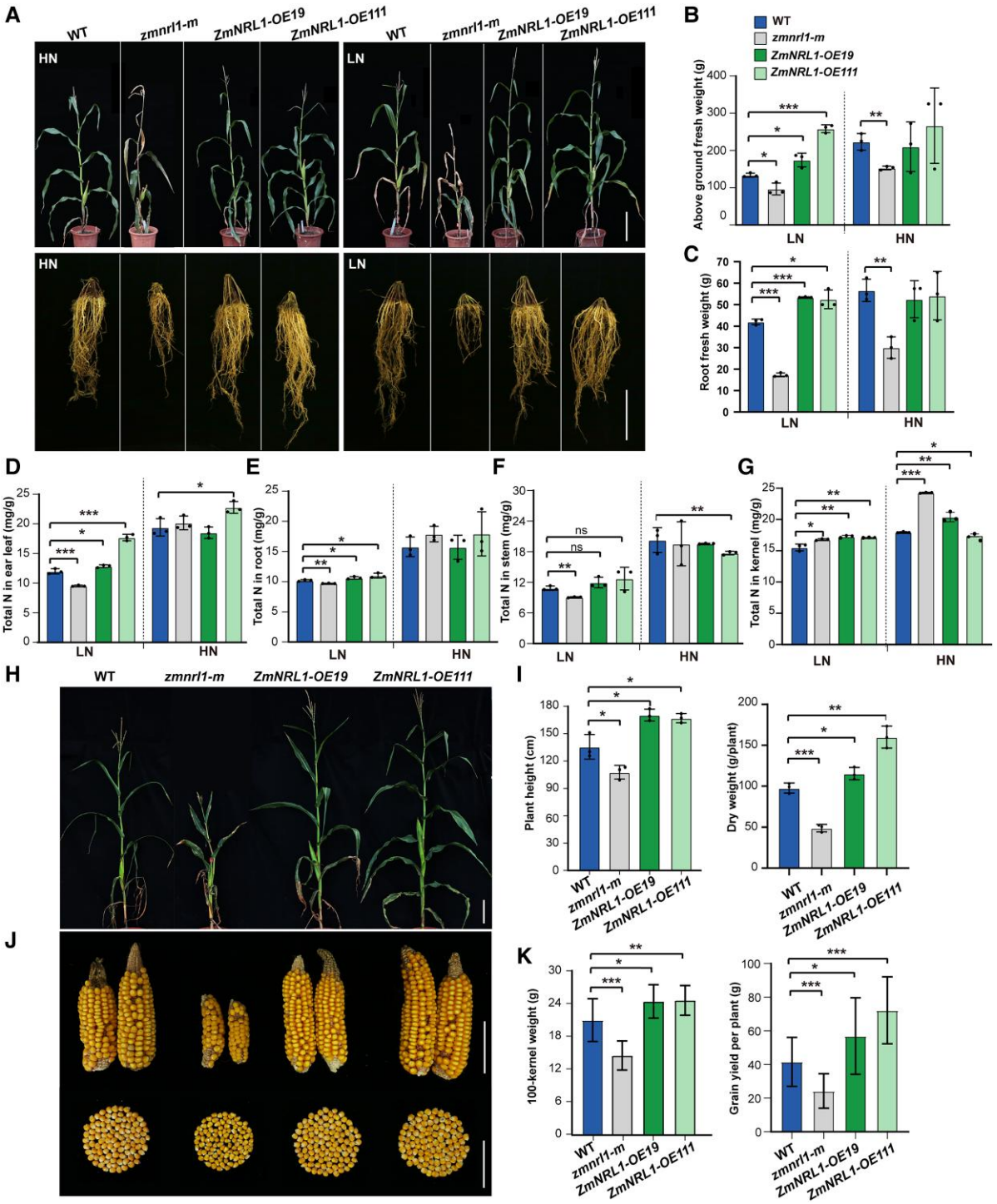

Fig. 8. *ZmNRL1* is essential for maize NUE and grain yield. (A) Phenotypic comparisons of wild type (WT), *zmnrl1-m* mutant, and *ZmNRL1*-overexpressing plants under low-N (0.15 mM NO_3^-) and high-N (15 mM NO_3^-) conditions. Bar, 40 cm (top); 15 cm (bottom). (B and C) Above-ground and root fresh weights of the WT, *zmnrl1-m*, and *ZmNRL1*-overexpressing lines under low-N and high-N conditions. (D-G) Quantitative analysis of total nitrogen content in ear leaves (D), roots (E), stems (F), and kernels (G). (H, J) Plant phenotype and typical ears of WT, *zmnrl1-m* mutant, and *ZmNRL1-OEs* plants under normal field conditions. Bar, 40 cm (H); 6 cm (J). (I, K) Comparisons of plant height and dry weight (I), 100-grain weight, and grain yield per plant (K) of WT, *zmnrl1-m*, and *ZmNRL1-OE* plants under normal field conditions. Values represent means ±SD; statistical significance was determined by two-sided *t*-test. Asterisks indicate a significant difference between the WT and the maize *ZmNRL1-OE* lines or *zmnrl1-m* lines: $^*P < 0.05$, $^{**}P < 0.01$, and $^{***}P < 0.001$.

ZmNRL1 using a constitutive promoter may improve the tolerance of Arabidopsis to N starvation. Therefore, we generated the Arabidopsis transgenic lines overexpressing ZmNRL1 tagged with HA (ZmNRL1-HA). The heterologous expression of *ZmNRL1* in two T_3 homozygous transgenic lines (*AtOE1* and *AtOE2*) was validated by qRT-PCR and western blotting, respectively (Supplementary Fig. S12A, B).

We then evaluated the tolerance of *AtOE* lines to N starvation in the seedling stage. As shown in Supplementary Fig. S12C and D, while there was no obvious phenotypic difference between *AtOE* and the non-transgenic wild type under N-rich conditions, *AtOE* seedlings shown better tolerance to N starvation than the wild type. Additionally, *AtOE* lines accumulated more nitrate and had higher NR activity in roots than those in the wild type (Supplementary Fig. S12E, G). Interestingly, higher nitrate and NR activity were found in leaves of *AtOE* lines under N-rich conditions as compared with the wild type (Supplementary Fig. S12F, H).

We also examined the phenotypic characteristics of soil-gown *AtOE* transgenic plants. These plants exhibited a similar growth rate to the wild type under normal growth conditions supplemented with N-rich fertilizer (5.5 mM NO_3^-). Interestingly, a significant increase in plant height at maturity was observed which, when compared with the wild type, was 9.7% and 4.4% higher for *AtOE1* and *AtOE2* plants, respectively (Supplementary Fig. S13A–D). In addition, *AtOE* lines exhibited an ~10% increase in seed weight (g of seeds per plant) compared with the wild type. *AtOE* lines also accumulated more proteins in the rosette leaves as compared with the wild type. Consistently, the expression levels of several key genes involved in N uptake and transport including *AtNRT1.1* and *AtNRT2.1*, as well as genes involved in N assimilation such as *AtNIR1* (*Nitrite reductase 1*), *AtNIA1* (*Nitrate reductase 1*), *AtGln2* (*Glutamine synthetase 2*), and *AtGlu1* (*Glutamate synthase 1*), were markedly up-regulated in *AtOE* transgenic plants (Supplementary Fig. S13E). When grown on soil continuously irrigated with N-deficient Hoagland solution for 5 weeks, *AtOE* lines showed better tolerance to N starvation with increased plant height and shoot DW per plant (Supplementary Fig. S12I–K) Together, these data indicated that overexpression of *ZmNRL1* in Arabidopsis improved its tolerance to N deficiency, as well as promoting plant growth and increasing seed yield under N-rich conditions.

Discussion

Crop growth and production rely heavily on N fertilizer in most intensive agricultural systems. However, excessive use of N fertilizer not only increases product costs but also results in serious environmental problems. Improving crop NUE offers a practical strategy to boost crop yields while reducing environmental pollution (Dong and Lin, 2020). Maize is a critically important source of food, feed, and energy globally (Andrews and Lea, 2013). However, the molecular mechanism(s) of N utilization and signalling in maize remain poorly understood. In this study, we identified a candidate gene, *ZmNRL1* (*Zm00001d019173*) associated with NUE-related traits based on GWAS, and demonstrated its role as a positive regulator of maize adaptation to N limitation.

CC is a common indicator of the N status of a plant. Using GWAS analysis, we identified an SNP within *ZmNRL1*, chr7.S_19754410, significantly associated with CC under N starvation. Re-sequencing a 4.7 kb genomic fragment containing *ZmNRL1* in 43 maize inbred lines from different geographic origins identified five more genetic variations in the coding region and 3′-UTR. The most significant variation, SNP642, is located in the first exon and has strong LD with the originally detected SNP1796/chr7.S_19754410 (Fig. 2). SNP642 is a non-synonymous variant with substitution of asparagine by aspartic acid, and SNP1796 is a silent polymorphism that does not cause a change in amino acid sequence. Based on these six variations, seven haplotypes were identified, which were further divided into two clades based on CC. Further expression analysis revealed that there is no significant difference in total *ZmNRL1* mRNA levels between the two clades (Figs 1, 2). It is not clear how the variants SNP642 and SNP1796 may confer a lower CC phenotype under N starvation. A likely explanation would be that they may influence factors such as protein structure/function, mRNA stability, and translation efficiency, and thus have significant biological consequences (Cannarozzi *et al.*, 2010; Rauscher and Ignatova, 2018; Y. Liu *et al.*, 2021). However, it cannot be excluded that these two SNPs are in LD with some other unidentified causal variant(s), which affects expression and/or function of *ZmNRL1* and thus confers a lower CC phenotype. Efforts directed at additional sequencing of untranslated and regulatory regions are needed, and a more comprehensive study using a larger sample size is required to examine whether the expression level of *ZmNRL1* is influenced by the SNPs.

ZmNRL1 belongs to a DUF630/632 domains-containing protein family with 26 members in the maize genome (Supplementary Fig. S4). To date, only a few genes of this family in Arabidopsis and rice have been studied, which revealed the important roles of DUF630/632 proteins in response to the changes in nutrient levels, as well as in multiple aspects of plant growth and development. The first characterized member, AtNRG2, functions in nitrate signaling in Arabidopsis, and its mutation disrupted the induction of many nitrate-responsive genes (Xu *et al.*, 2016). In addition, it regulates cadmium tolerance or allocation in Arabidopsis roots (Jian *et al.*, 2019). Another Arabidopsis member, AtAPSR1 (Altered Phosphate Starvation Response1), is required for root meristem maintenance under phosphate-limiting conditions and for modulating auxin distribution in the root tip (González-Mendoza *et al.*, 2013). As the closest homolog of AtNRG2 in rice (Supplementary Fig. S4), REL2 (Rolled and Erect Leaf 2) has been reported to regulate leaf rolling and morphology (Yang *et al.*, 2016). Three other alleles (*osdlt10*, *fgw1*, and *rsd1*) identified later further revealed the important roles of this DUF630/632 protein in tillering, grain filling, and stomatal development of

rice (Wen *et al.*, 2020; Yu *et al.*, 2020; Li *et al.*, 2023). In addition, *OsBBP1* (*OsbZIP72 binding protein 1*), another DUF630/632 domains-containing member in rice, was found to enhance drought resistance by modulating the balance of reactive oxygen species (Yu *et al.*, 2024).

Phylogenetic analysis showed that ZmNRL1 shared a clade with Arabidopsis AtNRG2 (Supplementary Fig. S4). Although they are similar, in this study, we showed that ZmNRL1 and AtNRG2 exhibit at least three differences in modulating N signaling. First, ZmNRL1 and AtNRG2 respond to the changes of nitrate levels in different fashions. AtNRG2 is required for the induction of nitrate-responsive genes (Xu *et al.*, 2016), whereas we demonstrated that ZmNRL1 regulates the expression of many N stress-induced genes in response to N starvation (Fig. 6). Second, the *atnrg2* mutant has no obvious morphological phenotype under low-nitrate conditions (Xu *et al.*, 2016), whereas the phenotypes of *zmnrl1* mutants are more evident under N-limiting conditions (Figs 3, 4). Third, AtNRG2 forms a complex with AtNLP7 in the nucleus, while ZmNRL1 is anchored to the plasma membrane through the putative N-myristoylation and palmitoylation motifs (Fig. 7) and does not interact with ZmNLPs (Supplementary Fig. S14). Thus, we speculate that the molecular mechanism by which ZmNRL1 mediates plant responses to N starvation is likely to differ from that of AtNRG2, and needs further studies.

Comparative RNA-seq analysis of the DEGs in the root under low-N stress showed that ZmNRL1 is required for the up-regulation of a set of key genes involved in N transport, assimilation, as well as signaling. They include genes encoding high-affinity nitrate transporter such as ZmNRT2.1 and ZmNRT2.2, ammonium transporters Zm00001d012261 and Zm00001d017249, amino acid permease Zm00001d017880, as well as regulators involved in N signaling such as ZmNLP3 and ZmCIPK23 (Han *et al.*, 2021) (Fig. 6; Supplementary Datasets S4, S6). Interestingly, our RNA-seq analysis also revealed that overexpression of *ZmNRL1* could further enhance the expression of genes involved in N assimilation such as *ZmASN2* (*Zm00001d044608*) and *ZmASN4* (*Zm00001d047736*), and the flavonoid metabolic process such as *ZmWHP1* (*Zm00001d007403*), *ZmFNS1* (*Zm00001d024946*), and *ZmC2* (*Zm00001d052673*) (Fig. 6; Supplementary Datasets S4, S6). The up-regulation of nitrate transporter (*AtNRT1.1* and *AtNRT2.1*) and nitrate utilization genes (*AtNIR1*, *AtNIA1*, *AtGln2*, and *AtGlu1*) was also observed in Arabidopsis overexpression lines (Supplementary Fig. S13E), which is consistent with the better tolerance of maize and Arabidopsis *ZmNRL1-OE* lines to N limitation (Fig. 5; Supplementary Fig. S12). According to the previous study by (Cao *et al.* 2017), the expression of *ZmNLP1-3* and *ZmNLP7* was induced by N starvation. In the present study, we found that the induction of *ZmNLP7* by N stress is independent of ZmNRL1, while the response of *ZmNLP3* and *ZmNLP1* to N starvation required the function of ZmNRL1, which further imply the critical role of ZmNRL1 in response to N stress.

Further analysis of the RNA-seq data directed our attention towards phosphate signaling. N and phosphorus (Pi) are the two mineral nutrients in the highest demand for plant growth. Therefore, coordinated utilization of both nutrients is essential for plants to attain nutrient balance and optimal growth. Recent studies have revealed that the nitrate-inducible transcriptional repressor AtNIGT1 coordinates the acquisition of both nutrients under fluctuating nutritional conditions in Arabidopsis (Kiba *et al.*, 2018), and that the OsNRT1.1B–OsSPX4 module in rice integrates the N and Pi signaling network (Hu *et al.*, 2019). Consistent with these studies, we found *ZmNIGT1.1* (*Zm00001d023411*) and *ZmNIGT1.2* (*Zm00001d023402*) in the list of N starvation down-regulated genes, as well as the Pi starvation signaling repressor *ZmSPX* (*Zm00001d017597*). In addition, three maize genes homologous to *AtPHR1* (PHOSPHATE STARVATION RESPONSE 1), the central Pi signaling regulator in Arabidopsis, were induced by N starvation. Among them, *Zm00001d015226* was up-regulated in a ZmNRL1-independent manner, while *Zm00001d003037* and *Zm00001d014701* were induced by N stress only in *ZmNRL1-OE* lines. In addition to PHR1, other TFs such as AtMYB62 and AtWRKY42 are reportedly involved in Pi starvation signaling (Devaiah *et al.*, 2009; Su *et al.*, 2015). The homologs to *AtMYB62* (*Zm00001d008528*) and *AtWRKY42* (*Zm00001d008190*) were also found to be up-regulated by N stress in *ZmNRL1-OE* plants (Fig. 6A; Supplementary Dataset S6). Collectively, we speculate that ZmNRL1 is a positive regulator in maize, modulating the responses not only to N stress but also to Pi starvation. It will be interesting to address which genes involved in N and Pi utilization are the direct targets of ZmNRL1, and future studies should thus be aimed at understanding to what extent ZmNRL1-dependent and ZmNRL1-independent mechanisms regulate N homeostasis in maize.

Supplementary data

The following supplementary data are available at *JXB* online.

Fig. S1. Analysis of six NUE-related traits in a maize natural population under N-starvation conditions.

Fig. S2. Manhattan and quantile–quantile (Q–Q) plots for NUE-related traits of maize.

Fig. S3. GWAS candidate gene analysis.

Fig. S4. Phylogenetic relationship and architecture of conserved protein motifs of ZmNRL1 homologous proteins.

Fig. S5. Gene expression profile of maize *ZmNRL1*.

Fig. S6. *zmnrl1* mutants used in this study.

Fig. S7. Phenotypes of soil-grown *zmnrl1* mutants under different nitrate concentrations.

Fig. S8. Leaf protein contents of the wild type and *zmnrl1* mutants under different nitrogen conditions.

Fig. S9. Tolerance of soil-grown *ZmNRL1* transgenic maize lines to N starvation.

Fig. S10. Transcriptomic analysis to identify genes regulated by ZmNRL1 during N starvation.

Fig. S11. The predicted *N*-myristoylation and palmitoylation sites in DUF630/632 domains-containing proteins of Arabidopsis and maize.

Fig. S12. Overexpression of *ZmNRL1* in Arabidopsis increases its tolerance to N starvation.
Fig. S13. Heterologous overexpression of *ZmNRL1* in Arabidopsis promotes plant growth.
Fig. S14. No protein–protein interaction between ZmNRL1 and ZmNLPs.
Table S1. The list of primers used in this study.
Table S2. NUE-related traits in a maize natural population under N starvation for 8 d.
Table S3. Phenotypic variance component and broad sense heritability of six NUE-related traits.
Table S4 SNPs and candidate genes significantly associated with NUE-related traits.
Table S5. GO annotation of 44 candidate genes performed by agriGO v2.0.
Table S6. List of 43 maize inbred lines for *ZmNRL1* re-sequencing.
Dataset S1. List of N starvation-up-regulated and -downregulated genes in the wild type.
Dataset S2. List of N starvation-up-regulated and -down-regulated genes in the *zmnrl1-m* mutant.
Dataset S3. List of N starvation-up-regulated and -down-regulated genes in *ZmNRL1-OE111*.
Dataset S4. GO enrichment analysis of N starvation-up-regulated genes in the wild type, *zmnrl1-m*, and *ZmNRL1-OE111*.
Dataset S5. GO enrichment analysis of N starvation-down-regulated genes in the wild-type, *zmnrl1-m*, and *ZmNRL1-OE111*.
Dataset S6. List of N starvation-up-regulated and -down-regulated representative genes in the wild type, *zmnrl1-m*, and *ZmNRL1-OE111* based on the Venn diagram.

Acknowledgements

We thank Professor Jianbing Yan of Huazhong Agricultural University for providing the seeds of the maize AM368 population and SNP data support, Professor Xiaohong Yang of China Agricultural University and Professor Xiangguo Liu of Jilin Academy of Agricultural Sciences for maize materials, Professor Haiyang Wang of South China Agricultural University (SCAU) for kindly providing the *CPB-Ubipro: GFP* vector, and Professor Caiji Gao of South China Normal University for the *pGreenII 0229* vector. We thank SCAU colleagues Jiang Tian, Jun Huang, and Dexin Kong for technical assistance and reagents. We also thank the Instrumental Analysis & Research Center of SCAU for technical assistance with the element analyzer.

Author contributions

FL, NL, and CZ: study design; CZ, HL, YL, XH, and JH: performed the experiments; CZ, HL, and FL: analyzed the transcriptomic data; CZ, JH, and NL: performed the GWAS analysis; CZ and FL; analyzed the data and wrote the manuscript. All authors read and approved the manuscript.

Conflict of interest

The authors declare no competing financial interests.

Funding

This work was supported by the National Natural Science Foundation of China (grant No. 32300226 to CZ and 31970307 to FL), the open competition program of top ten critical priorities of Agricultural Science and Technology Innovation for the 14th Five-Year Plan of Guangdong Province (grant no. 2022SDZG05 to FL), and China Postdoctoral Science Foundation (grant no. 2022M721205 to CZ).

Data availability

The published RNA-sequencing data (SRP139303) are retrieved from the NCBI Sequence Read Archive database. The raw reads and raw counts for the RNA-seq datasets in this study are available at National Center for Biotechnology Information Gene Expression Omnibus (GEO) with accession number GSE252822. The maize association panel of 368 various populations is taken from the MaizeGo website (www.maizego.org/Resources.html). All data supporting the findings of this study are available within the paper and within its supplementary data published online.

References

Alvarez JM, Riveras E, Vidal EA, *et al.* 2014. Systems approach identifies TGA1 and TGA4 transcription factors as important regulatory components of the nitrate response of *Arabidopsis thaliana* roots. The Plant Journal **80**, 1-13.

Alvarez JM, Schinke AL, Brooks MD, Pasquino A, Leonelli L, Varala K, Safi A, Krouk G, Krapp A, Coruzzi GM. 2020. Transient genome-wide interactions of the master transcription factor NLP7 initiate a rapid nitrogen-response cascade. Nature Communications **11**, 1157.

Andrews M, Lea PJ. 2013. Our nitrogen 'footprint': the need for increased crop nitrogen use efficiency. Annals of Applied Biology **163**, 165-169.

Bradbury PJ, Zhang Z, Kroon DE, Casstevens TM, Ramdoss Y, Buckler ES. 2007. TASSEL: software for association mapping of complex traits in diverse samples. Bioinformatics **23**, 2633-2635.

Bradford MM. 1976. A rapid and sensitive method for the quantitation of microgram quantities of protein utilizing the principle of protein-dye binding. Analytical Biochemistry **72**, 248-254.

Cannarozzi G, Schraudolph NN, Faty M, von Rohr P, Friberg MT, Roth AC, Gonnet P, Gonnet G, Barral Y. 2010. A role for codon order in translation dynamics. Cell **141**, 355-367.

Cao H, Liu Z, Guo J, *et al.* 2024. ZmNRT1.1B (ZmNPF6.6) determines nitrogen use efficiency via regulation of nitrate transport and signalling in maize. Plant Biotechnology Journal **22**, 316-329.

Cao H, Qi S, Sun M, Li Z, Yang Y, Crawford NM, Wang Y. 2017. Overexpression of the maize *ZmNLP6* and *ZmNLP8* can complement the *Arabidopsis* nitrate regulatory mutant *nlp7* by restoring nitrate signaling and assimilation. Frontiers in Plant Science **8**, 1703.

Clough SJ, Bent AF. 1998. Floral dip: a simplified method for *Agrobacterium*-mediated transformation of *Arabidopsis thaliana*. The Plant Journal **16**, 735-743.

Coskun D, Britto DT, Shi W, Kronzucker HJ. 2017. Nitrogen transformations in modern agriculture and the role of biological nitrification inhibition. Nature Plants **3**, 17074.

Devaiah BN, Madhuvanthi R, Karthikeyan AS, Raghothama KG. 2009. Phosphate starvation responses and gibberellic acid biosynthesis are regulated by the MYB62 transcription factor in *Arabidopsis*. Molecular Plant **2**, 43-58.

Dong NQ, Lin HX. 2020. Higher yield with less nitrogen fertilizer. Nature Plants **6**, 1078-1079.

Fu J, Cheng Y, Linghu J, *et al.* 2013. RNA sequencing reveals the complex regulatory network in the maize kernel. Nature Communications **4**, 2832.

Ge M, Wang Y, Liu Y, *et al.* 2020. The NIN-like protein 5 (ZmNLP5) transcription factor is involved in modulating the nitrogen response in maize. The Plant Journal **102**, 353-368.

González-Mendoza V, Zurita-Silva A, Sánchez-Calderón L, Sánchez-Sandoval ME, Oropeza-Aburto A, Gutiérrez-Alanís D, Alatorre-Cobos F, Herrera-Estrella L. 2013. *APSR1*, a novel gene required for meristem maintenance, is negatively regulated by low phosphate availability. Plant Science **205-206**, 2-12.

Guo JH, Liu XJ, Zhang Y, *et al.* 2010. Significant acidification in major Chinese croplands. Science **327**, 1008-1010.

Guo L, Li H, Cao X, Cao A, Huang M. 2021. Effect of agricultural subsidies on the use of chemical fertilizer. Journal of Environmental Management **299**, 113621.

Han W, Ji Y, Wu W, Cheng JK, Feng HQ, Wang Y. 2021. ZMK1 is involved in K^+ uptake and regulated by protein kinase ZmCIPK23 in *Zea mays*. Frontiers in Plant Science **12**, 517742.

Ho CH, Lin SH, Hu HC, Tsay YF. 2009. CHL1 functions as a nitrate sensor in plants. Cell **138**, 1184-1194.

Hu B, Jiang Z, Wang W, *et al.* 2019. Nitrate-NRT1.1B-SPX4 cascade integrates nitrogen and phosphorus signalling networks in plants. Nature Plants **5**, 401-413.

Huang S, Yang W, Ding W, Jia L, Jiang L, Liu Y, Xu X, Yang Y, He P, Yang J. 2021. Estimation of nitrogen supply for summer maize production through a long-term field trial in China. Agronomy **11**, 1358.

Ishida Y, Hiei Y, Komari T. 2007. *Agrobacterium*-mediated transformation of maize. Nature Protocols **2**, 1614-1621.

Jian S, Luo J, Liao Q, Liu Q, Guan C, Zhang Z. 2019. *NRT1.1* regulates nitrate allocation and cadmium tolerance in *Arabidopsis*. Frontiers in Plant Science **10**, 384.

Kiba T, Inaba J, Kudo T, *et al.* 2018. Repression of nitrogen starvation responses by members of the *Arabidopsis* GARP-type transcription factor NIGT1/HRS1 subfamily. The Plant Cell **30**, 925-945.

Krapp A. 2015. Plant nitrogen assimilation and its regulation: a complex puzzle with missing pieces. Current Opinion in Plant Biology **25**, 115-122.

Krouk G, Mirowski P, LeCun Y, Shasha DE, Coruzzi GM. 2010. Predictive network modeling of the high-resolution dynamic plant transcriptome in response to nitrate. Genome Biology **11**, R123.

Ladha JK, Tirol-Padre A, Reddy CK, Cassman KG, Verma S, Powlson DS, van Kessel C, de B Richter D, Chakraborty D, Pathak H. 2016. Global nitrogen budgets in cereals: a 50-year assessment for maize, rice, and wheat production systems. Scientific Reports **6**, 19355.

Lassaletta L, Billen G, Grizzetti B, Anglade J, Garnier J. 2014. 50 year trends in nitrogen use efficiency of world cropping systems: the relationship between yield and nitrogen input to cropland. Environmental Research Letters **9**, 105011.

Li F, Chung T, Pennington JG, Federico ML, Kaeppler HF, Kaeppler SM, Otegui MS, Vierstra RD. 2015. Autophagic recycling plays a central role in maize nitrogen remobilization. The Plant Cell **27**, 1389-1408.

Li S, Ji M, Liu F, Zhu M, Yang Y, Zhang W, Liu S, Wang Y, Lv W, Qi S. 2024. NRG2 family members of *Arabidopsis* and maize regulate nitrate signalling and promote nitrogen use efficiency. Physiologia Plantarum **176**, e14251.

Li Y, He P, Wang X, Chen H, Ni J, Tian W, Zhang X, Cui Z, He G, Sang X. 2023. FGW1, a protein containing DUF630 and DUF632 domains, regulates grain size and filling in *Oryza sativa* L. The Crop Journal **11**, 1390-1400.

Liang L, Zhou L, Tang Y, *et al.* 2019. A sequence-indexed mutator insertional library for maize functional genomics study. Plant Physiology **181**, 1404-1414.

Liu KH, Niu Y, Konishi M, *et al.* 2017. Discovery of nitrate-CPK-NLP signalling in central nutrient-growth networks. Nature **545**, 311-316.

Liu KH, Liu M, Lin Z, *et al.* 2022. NIN-like protein 7 transcription factor is a plant nitrate sensor. Science **377**, 1419-1425.

Liu Y, Yang Q, Zhao F. 2021. Synonymous but not silent: the codon usage code for gene expression and protein folding. Annual Review of Biochemistry **90**, 375-401.

Liu YQ, Wang H, Jiang Z, *et al.* 2021. Genomic basis of geographical adaptation to soil nitrogen in rice. Nature **590**, 600-605.

Lu X, Liu J, Ren W, *et al.* 2018. Gene-indexed mutations in maize. Molecular Plant **11**, 496-504.

Luo N, Shang D, Tang Z, *et al.* 2023. Engineered ATG8-binding motif-based selective autophagy to degrade proteins and organelles in planta. New Phytologist **237**, 684-697.

Marchive C, Roudier F, Castaings L, Bréhaut V, Blondet E, Colot V, Meyer C, Krapp A. 2013. Nuclear retention of the transcription factor NLP7 orchestrates the early response to nitrate in plants. Nature Communications **4**, 1713.

McLoughlin F, Augustine RC, Marshall RS, Li F, Kirkpatrick LD, Otegui MS, Vierstra RD. 2018. Maize multi-omics reveal roles for autophagic recycling in proteome remodelling and lipid turnover. Nature Plants **4**, 1056-1070.

Palacios-Rojas N, McCulley L, Kaeppler M, Titcomb TJ, Gunaratna NS, Lopez-Ridaura S, Tanumihardjo SA. 2020. Mining maize diversity and improving its nutritional aspects within agro-food systems. Comprehensive Reviews in Food Science and Food Safety **19**, 1809-1834.

Rauscher R, Ignatova Z. 2018. Timing during translation matters: synonymous mutations in human pathologies influence protein folding and function. Biochemical Society Transactions **46**, 937-944.

Rubin G, Tohge T, Matsuda F, Saito K, Scheible WR. 2009. Members of the LBD family of transcription factors repress anthocyanin synthesis and affect additional nitrogen responses in *Arabidopsis*. The Plant Cell **21**, 3567-3584.

Su T, Xu Q, Zhang FC, Chen Y, Li LQ, Wu WH, Chen YF. 2015. WRKY42 modulates phosphate homeostasis through regulating phosphate translocation and acquisition in *Arabidopsis*. Plant Physiology **167**, 1579-1591.

Tsay YF, Schroeder JI, Feldmann KA, Crawford NM. 1993. The herbicide sensitivity gene *CHL1* of Arabidopsis encodes a nitrate-inducible nitrate transporter. Cell **72**, 705-713.

Vidal EA, Álvarez JM, Gutiérrez RA. 2014. Nitrate regulation of *AFB3* and *NAC4* gene expression in *Arabidopsis* roots depends on NRT1.1 nitrate transport function. Plant Signaling & Behavior **9**, e28501.

Vidal EA, Alvarez JM, Araus V, *et al.* 2020. Nitrate in 2020: thirty years from transport to signaling networks. The Plant Cell **32**, 2094-2119.

Wang R, Liu D, Crawford NM. 1998. The *Arabidopsis* CHL1 protein plays a major role in high-affinity nitrate uptake. Proceedings of the National Academy of Sciences, USA **95**, 15134-15139.

Wen X, Sun L, Chen Y, *et al.* 2020. Rice *dwarf and low tillering 10* (*OsDLT10*) regulates tiller number by monitoring auxin homeostasis. Plant Science **297**, 110502.

Wu J, Zhang ZS, Xia JQ, *et al.* 2021. Rice NIN-LIKE PROTEIN 4 plays a pivotal role in nitrogen use efficiency. Plant Biotechnology Journal **19**, 448-461.

Xu G, Fan X, Miller AJ. 2012. Plant nitrogen assimilation and use efficiency. Annual Review of Plant Biology **63**, 153-182.

Xu G, Takahashi H. 2020. Improving nitrogen use efficiency: from cells to plant systems. Journal of Experimental Botany **71**, 4359-4364.

Xu N, Wang R, Zhao L, *et al.* 2016. The *Arabidopsis* NRG2 protein mediates nitrate signaling and interacts with and regulates key nitrate regulators. The Plant Cell **28**, 485-504.

Yang SQ, Li WQ, Miao H, Gan PF, Qiao L, Chang YL, Shi CH, Chen KM. 2016. *REL2*, a gene encoding an unknown function protein which contains DUF630 and DUF632 domains controls leaf rolling in rice. Rice (NY) **9**, 37.

Yang X, Gao S, Xu S, Zhang Z, Prasanna BM, Li L, Li J, Yan J. 2011. Characterization of a global germplasm collection and its potential utilization for analysis of complex quantitative traits in maize. Molecular Breeding **28**, 511-526.

Yin L, Zhang H, Tang Z, *et al.* 2021. rMVP: a memory-efficient, visualization-enhanced, and parallel-accelerated tool for genome-wide association study. Genomics, Proteomics & Bioinformatics **19**, 619-628.

Yu Q, Chen L, Zhou W, An Y, Luo T, Wu Z, Wang Y, Xi Y, Yan L, Hou S. 2020. *RSD1* is essential for stomatal patterning and files in rice. Frontiers in Plant Science **11**, 600021.

Yu X, Wang L, Xie Y, *et al.* 2024. OsBBP1, a newly identified protein containing DUF630 and DUF632 domains confers drought tolerance in rice. Plant Science **345**, 112119.

Yuan Z, Ata-Ul-Karim ST, Cao Q, Lu Z, Cao W, Zhu Y, Liu X. 2016. Indicators for diagnosing nitrogen status of rice based on chlorophyll meter readings. Field Crops Research **185**, 12-20.

Zhao Y, Zhao B, Xie Y, *et al.* 2023. The evening complex promotes maize flowering and adaptation to temperate regions. The Plant Cell **35**, 369-389.